

DESIGN, MODELLING, PERFORMANCE OPTIMIZATION AND EXPERIMENTATION OF A REVERSIBLE HP/ORC PROTOTYPE

*Olivier, Dumont, PhD student, Thermodynamics and Energetics Laboratory
Chemin des chevreuils, 7 (B49), 4000 Liege, Belgium*

*Sylvain, Quoilin, Post-doctoral research associate, Thermodynamics and Energetics
Laboratory Chemin des chevreuils, 7 (B49), 4000 Liege, Belgium*

*Vincent, Lemort, Professor, Thermodynamics and Energetics Laboratory
Chemin des chevreuils, 7 (B49), 4000 Liege, Belgium*

Abstract: This paper presents an innovative system comprising a water/water heat pump connected to a solar roof and a geothermal heat exchanger. This unit is able to invert its cycle and operate as an Organic Rankine Cycle. The solar roof is producing a large amount of heat throughout the year. This allows covering the building annual heating needs and furthermore, electricity is produced thanks to the surplus of heat in a so-called HP/ORC reversible unit. This paper is focusing on these three main points: modeling, design and experimentation of the prototype. This paper demonstrates the feasibility of such a prototype with encouraging performance in ORC and HP modes. First simulations of the HP/ORC system, with components optimally sized, indicate that, in ORC mode, for the weather conditions of Copenhagen, the electrical energy produced over one year reaches 4030 kWh and the nominal efficiency of the cycle is 7.6%. The nominal COP of the heat pump is 4.2 (condenser exhaust temperature of 60°C and evaporator supply temperature of 15°C). Experimentally, a COP of 4.21 (condensation temperature of 61°C and evaporation temperature of 21°C) is achieved in heat pump mode and a global ORC efficiency of 5.7% is obtained in ORC mode (condenser exhaust temperature of 25°C and evaporator supply temperature of 88°C)..

Key Words: Heat pump, ORC, modeling, Scroll compressor, reversible

1 INTRODUCTION

A important sector where measures must be adopted to significantly reduce energy consumption and greenhouse gases emissions is the building sector (37% of the total final energy consumption of the EU (Perez et al 2008)). In this context, heat pumps provides energy-efficient space and domestic hot water heating in many applications (Hepbasli 2009, Georges 2013). This paper presents an innovative system comprising a water/water heat pump connected to a solar roof and a geothermal heat exchanger (Figure 1). This heat pump is reversible, meaning that it can be run as an Organic Rankine Cycle (ORC). A large amount of heat (sometimes more than 100 kW) is generated throughout the year by the solar roof. This heat is used in priority to cover the building heating needs and the surplus heat generated is utilized in a so-called HP/ORC module to generate electricity. It also works as an efficient heat pump which simplifies the complexity of the total system compared to competitive products (heat pump combined with photovoltaics for example).

There is only one reference exploring this concept in literature (Schimpf 2013). It focuses on yearly simulation and thermo-economic feasibility of the system in a classical house with

accurate models for solar collectors, heat storage and ground heat exchanger. The concept presented in this paper is different from Schimpf's work because the house (ground heat exchanger and solar absorber) is built around the module for a better integration. This leads to a larger solar roof (15 times larger) and a longer ground heat exchanger that allows to produce much more electricity through the year. The prototype is already built and installed in the house in Herring (Denmark) and is working nowadays (Innogie 2013).

This paper is organized as follows: First a short description of the concept with the three different operating modes is done. After that, the modeling of each component is detailed and a complete sizing model is developed. This model is used to assess the performance of the system in both ORC and HP modes. Finally, results from experimentation are described.

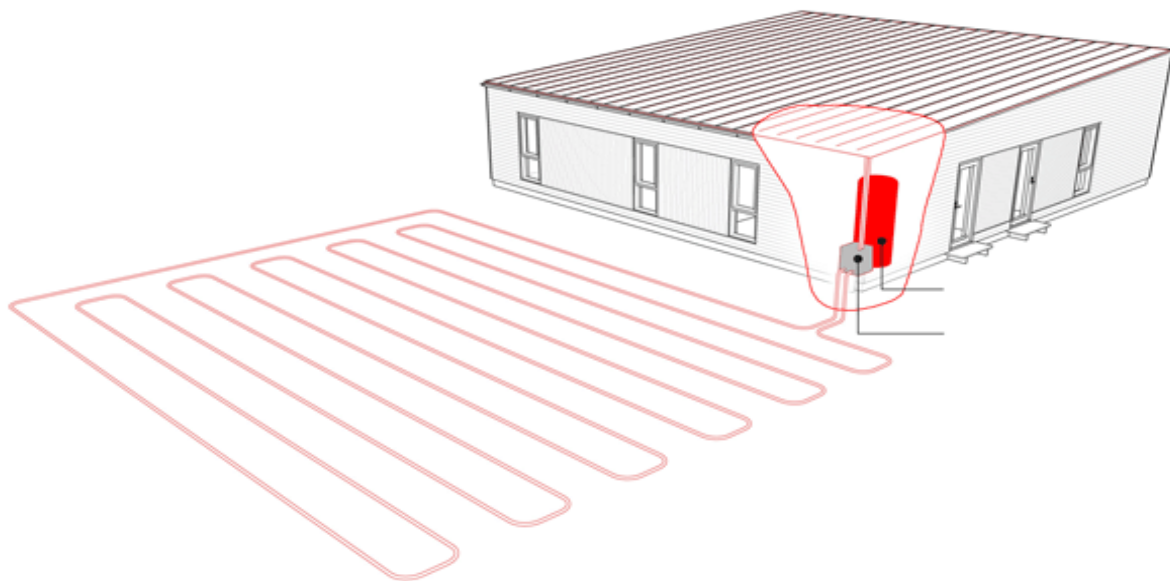


Figure 1: The reversible HP/ORC unit integrated into the house with a solar absorber and the ground heat exchanger (Innogie 2013)

2 WORKING PRINCIPLE

2.1.1 Organic Rankine Cycle mode

When the heating requirements of the house are covered by the heat storage and that the weather conditions are appropriate, the ORC mode is used to generate electricity (Figure 2). The working process is relatively simple: heat coming from the roof evaporates the working fluid through the evaporator. Then, the working fluid expands in the scroll device generating electricity. Following this, the refrigerant (R134a) is condensed thanks to the ground heat exchanger and goes into the pump before starting the cycle again.

2.1.2 Heat Pump mode

When heating requirements of the house cannot be covered by the heat storage or by the direct heating mode, the heat pump mode is activated. The components necessary to use the heat pump are almost the same as the ORC mode except that the pump is bypassed by an electronic expansion valve and that the condenser is connected to the heat storage. It works as a classical water to water heat pump, with its evaporator connected to the solar roof.

2.1.3 Direct heating mode

This mode is used as long as the heat storage cannot cover the heat requirements and provided that the heat transfer rate exchanged with the roof is sufficient. The heat goes from the solar absorber to the heat storage through a heat exchanger.

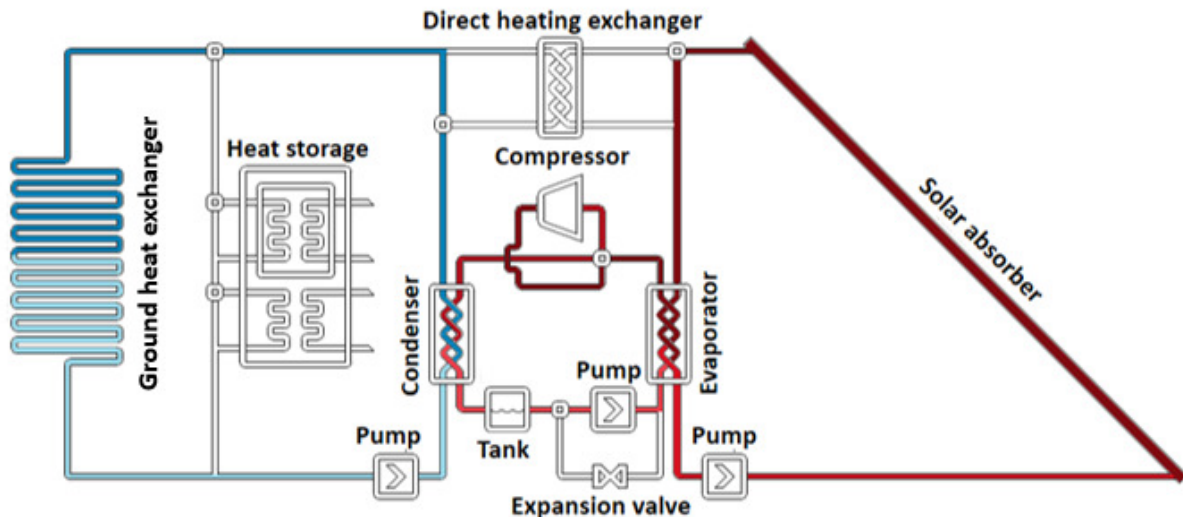


Figure 2: Reversible HP/ORC detailed scheme (ORC mode)

3 MODELLING

3.1 Compressor - expander

The machine used as an expander or as a compressor following the operating mode is a modified scroll compressor. This choice has been based on the ability of this machine to work in both mode and because this is the more efficient expansion device for low power (<10kWel) solar applications (Quoilin 2011). The compressor is simulated by empirical correlation from the manufacturer (Emerson 2013) following European standard (European standard 1999). There are no efficiency data available for the expander mode from the manufacturer. A semi-empirical model, proposed by (Lemort 2008) and validated by tests with R245fa (Lemort et al 2011) is used. The model requires only nine parameters (heat transfer coefficients, friction torque, leakage area and pressure drop equivalent diameter). They are scaled with the laws proposed by (Lemort 2008).

3.2 Exchangers

Plate heat exchangers are chosen for the condenser, evaporator and direct heating exchanger because they present good efficiencies, compactness's and prices. A three zones model is considered. Heat transfer coefficients are evaluated with Thonon's correlation for single phase zones (Thonon 1995), with Kuo's correlation for condensation (Kuo 2005) and with Hsieh's correlation for evaporation (Hsieh 2002). These models are validated with R410 and are used for R134a in this paper because models for plate heat exchangers are very scarce and because results diverge from one to another (Garcia-Cascales, 2007). In the sizing model, the surface and the number of plates are evaluated trough an imposed pinch-point and a maximum pressure drop on refrigerant side (Quoilin 2011). The surface and the number of plates are of course imposed in the simulation model.

3.3 Solar roof

The roof is modeled by a simple linear model (Innogie 2013) because this work is more focused on the HP/ORC unit. S_{abs} is the total absorber area (150 m²), $\eta_{glazing}$ is the optical efficiency, i.e. the transmissivity, (88%), T_{amb} is the ambient temperature, I is the current solar insolation (in W/m²) and ΔT_{abs} is the difference between the ambient temperature and the average heat transfer fluid temperature in the collector.

$$\dot{Q}_{abs} [W] = S_{abs} (-26.2 - 1.22T_{amb} - 1.7 \Delta T_{abs} + 0.903 I) \quad (1)$$

$$\eta_{abs} [-] = \frac{\dot{Q}_{abs} \cdot \eta_{glazing}}{I \cdot S_{abs}} \quad (2)$$

3.4 Storage

A model of storage including ambient losses (Q_{sto}) is used (Delta calor, 2013). The volume (V_{sto}) and the storage temperature (T_{sto}) are imposed at 1000 litres and 55°C respectively.

$$Q_{sto} \left[\frac{Wh}{day} \right] = 4,2 \cdot V_{sto}^{0,47} \cdot (T_{sto} - T_{amb}) \quad (3)$$

3.5 Pump

Constraints on the flow in ORC mode - relatively high pressure drops (≈ 20 bar) and low flow (≈ 300 g/s) – leads to the use of a volumetric pump. A plunger pump is chosen based on its efficiency, price and tightness. The pump is modeled with a constant isentropic efficiency (ϵ_{is}) of 0.5 (Equation 5). This allows to evaluate the electrical consumption of the pump (\dot{W}_{pp}). \dot{m} is the mass flow, $h_{ex,is}$ is the isentropic enthalpy at the exhaust of the pump and h_{su} is the supply enthalpy of the pump.

$$\epsilon_{is} [-] = \frac{\dot{m} (h_{ex,is} - h_{su})}{\dot{W}_{pp}} \quad (5)$$

4 SIZING

4.1 Definition of the nominal conditions

Since all the components models are detailed, nominal conditions are necessary to size our components. The ORC mode is the one involving the highest heat flow exchanged with the heat source and sink, it is therefore the one selected for the sizing of the system components.

The nominal sizing conditions are defined as follows:

- The evaporating temperature is set to 90°C, which approximately corresponds to the maximum pressure at the inlet of the expander (32 bars) with the selected fluid.
- On the cooling water side, an inlet temperature of 15°C and an outlet temperature of 20°C are assumed.
- The heat source temperature glide, i.e. the difference between the inlet and outlet glycol water temperature on the absorber, is set to 25K in order to conserve a reasonable glycol water flow rate.
- The pinch points are set to 5K for the evaporator and 7.5K for the condenser (Quoilin et al 2011).

- The superheating and sub-cooling of the evaporator and the condenser are set to 10K and 2K respectively.

For the heat pump mode, the following operating conditions are imposed:

- The evaporating temperature (15,7°C) is selected as the equilibrium temperature when the heat pump heating capacity is 8 kWth and when the solar radiation is 90 W/m². This is representative of winter conditions in Denmark.

- The glycol water flow rate (evaporator) is set to the value provided by the ORC mode, depending on the scroll machine power.

- The condensing temperature is fixed to 60°C in order to get a water temperature around 55°C at the inlet of the heat storage (value chosen to be conservative). This temperature is sufficient to cover all the needs of the house.

- For hot water production, a temperature difference of 5K is assumed between the inlet and the outlet of the condenser.

- The superheating and sub-cooling of the evaporator and the condenser are set to 3K and 2K respectively.

The heat exchangers and the pump are sized using the nominal summer conditions. However, the size of the scroll machine (which defines the net power of the system, both in HP and ORC mode) results from a tradeoff between winter and summer performance. This can only be optimized using yearly simulations, as proposed in the section 4.2. The results presented in Table 1 for the nominal conditions have been obtained with the optimal expander size (swept volume = 98.04 cm³) and the optimal fluid (R134a) resulting from yearly simulation optimization (see section 4.2).

Table 1: Nominal conditions

| Mode | Parameter | Value |
|-----------|--------------------------------------|-------|
| Heat pump | Evaporation pressure [bar] | 5 |
| | Condensation pressure [bar] | 17 |
| | Power consumed [W] | 3211 |
| | Mass flow[kg/s] | 0.1 |
| | Compressor isentropic efficiency [%] | 60 |
| | Absorber efficiency [%] | 56 |
| | COP [-] | 4.2 |
| ORC | Evaporation pressure [bar] | 33 |
| | Condensation pressure [bar] | 7 |
| | Power produced [W] | 4733 |
| | Mass flow[kg/s] | 0.3 |
| | Expander isentropic efficiency [%] | 68 |
| | Absorber efficiency [%] | 55 |
| | ORC global efficiency [%] | 7.6 |

4.2 Yearly simulations

In the previous section, the performance of the system has been evaluated on a nominal sizing point, allowing to select and to define the geometry of some components. However when optimizing the design, it is important to account for the performance of the system over a whole year. The system is therefore simulated over a whole year (with one hour time step) by taking into account the average climatic conditions, the average building heat demand for each month of the year and the control strategy. The outside temperature and the solar irradiance are inputs based on Copenhagen since the unit is installed in Denmark. The following control strategy is used: The ORC mode is used as long as the heat storage can

cover the heat demand. If this is not the case, the direct heating mode is activated. Finally, the HP mode is selected for severe climate conditions when the direct heating mode does not allow reaching the required heating temperature.

These simulations allow optimizing discrete variables such as the choice of the working fluid, the use of a recuperator, and the size of the scroll machine (available sizes are taken from the catalog of one manufacturer). The following methodology is applied:

1. For a given configuration (fluid, expander size, recuperator or not), the condenser and of the evaporator are re-sized in term of area and number of plates and the system performance is evaluated over a wide range of evaporation/condensation temperatures, both for the ORC mode and the HP mode. This is done with the nominal condition methodology (see section 4.1).
2. Performance curves are derived from these simulations as a function of the system configuration and of the temperature levels.
3. These curves are implemented in the yearly simulation model, which optimally switches between the three operating modes depending on the weather conditions and on the heat demand.

Point 2 is achieved by running the simulation model for different mean absorber temperatures in order to see the evolution of the electrical power and the heat transfer to the evaporator. In this example, the performance of three compressors (A, B and C) are compared. Technical data is presented in Table 2. This curves are shown for the ORC mode (Figure 3) and for the HP mode (Figure 4).

Table 2: Technical data of the three compressors

| Compressor Parameter | Case A | Case B | Case C |
|------------------------|--------|--------|--------|
| Swept volume [-] | 82.6 | 98.04 | 119.96 |
| Volume ratio [-] | ≈ 3 | ≈ 3 | ≈ 3 |
| Maximum pressure [bar] | 32 | 32 | 32 |

For the ORC mode, the power transferred (\dot{Q}_{ev} continuous line – Figure 3) increases when the mean absorber temperature (\bar{T}) rises and thus net output power (\dot{W}_{net}) increases too. This is due to the fact that the evaporating temperature and pressure increase when the hot source temperature rises, hot source flow rate being constant. However it is important not to exceed the maximum pressure at the expander inlet. This involves a limitation on the power generation. Though, in order to increase the electrical power when the maximum pressure is reached, the pressure is fixed at its maximum value and the super-heating is increased. This explains the discontinuity appearing around 95°C. It can be seen that when the maximum pressure is reached, increasing the superheating involves a decrease in the thermal power transferred (continuous lines) but it allows increasing still a bit more the power produced (dashed lines). From these curves, polynomial laws have been fitted in order to perform the yearly simulation:

$$\dot{Q}_{ev} = C_0 + C_1 \cdot \bar{T} + C_2 \cdot \bar{T}^2 \quad (6)$$

$$\dot{W}_{net} = K_0 + K_1 \cdot \bar{T} + K_2 \cdot \bar{T}^2 \quad (7)$$

For the next step, in the yearly simulation, the mean glycol water temperature will be computed from the weather data (ambient temperature and solar radiation) and from the polynomial expression of the thermal power transferred (Equation 8). This will therefore allow determining the mean absorber temperature corresponding to the weather data and then, the related power generation and the performance of the system in the ORC mode.

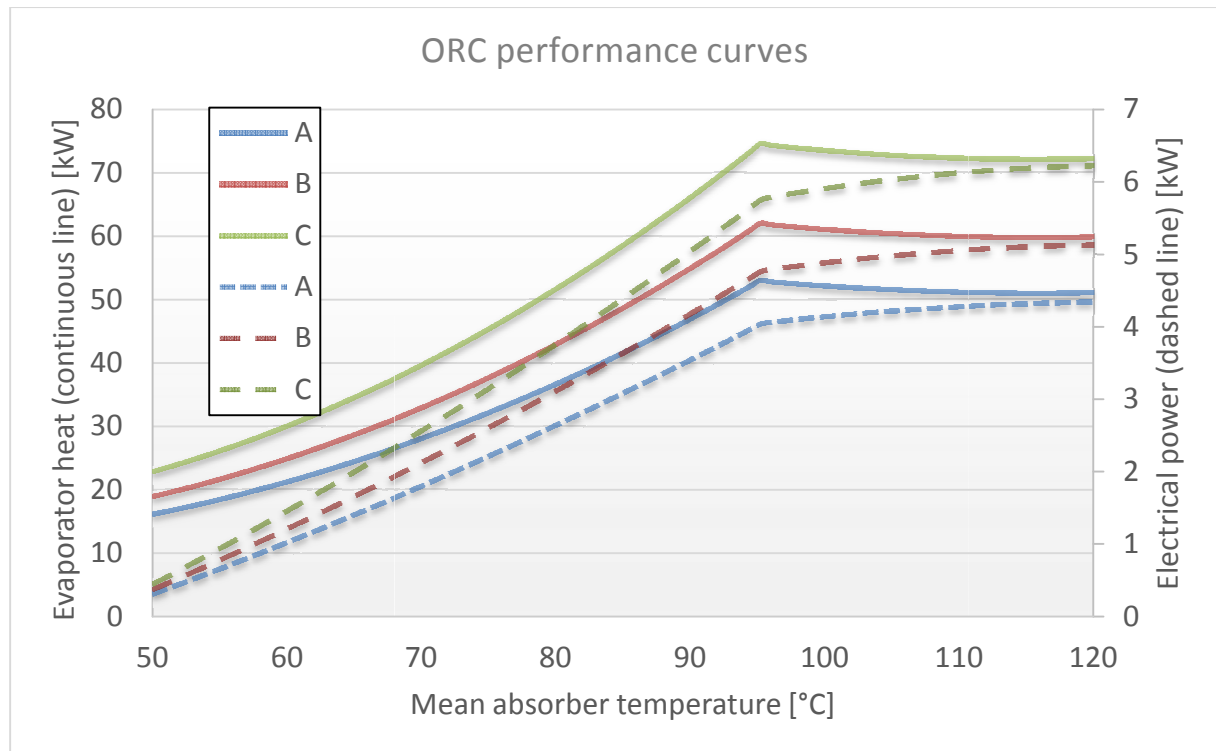


Figure 3: ORC performance curves in function of the mean absorber temperature

In heat pump mode, the sizing of the exchangers is the same as in ORC mode because the thermal power is higher. The simulation model has been run for different mean absorber temperatures in order to see the evolution of the electrical power consumption with the thermal power transferred to the evaporator and operating conditions (Figure 4). The thermal power transferred to the evaporator () and the electrical power consumption () increases when the mean absorber temperature rises. The thermal power recovered at the condenser () increases therefore too because the energy balance on the heat pump gives:

$$(8)$$

Moreover, as the ORC mode, polynomial laws have been derived from these curves for yearly simulations. The weather conditions combined with these polynomial expressions will allow us to determine the mean absorber temperature, the thermal power recovered at the condenser and the performance of the heat pump.

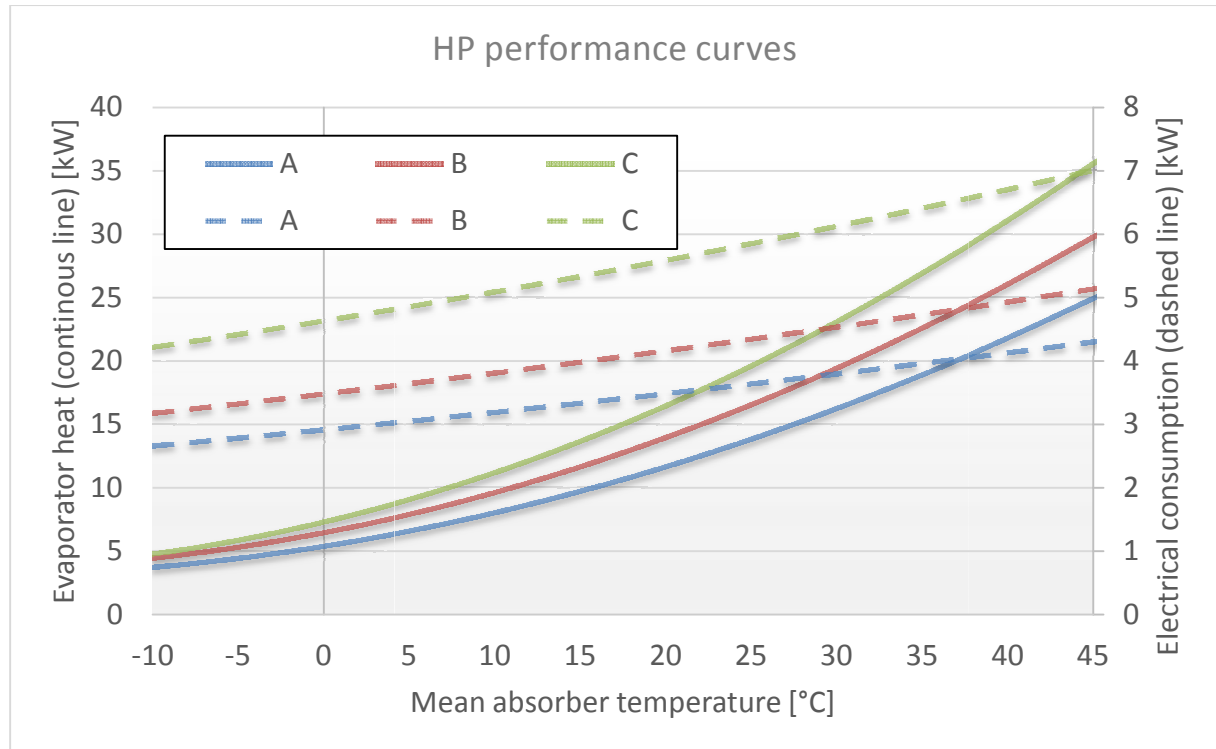


Figure 4: HP performance curves in function of the mean absorber temperature

Finally, the addition of the heat demand of the house and the thermal losses of the heat storage gives the total energy that the unit needs to produce.

Table 3 presents the results in terms of electrical power and running time from these yearly simulation in the case of compressor B and with the optimum fluid (see section 4.3). The heat pump mode is only used during 3 months. The rest of the year, the direct heating is sufficient to provide the heat required by the building and the ORC mode allows producing electricity with the surplus heat.

Table 3: Electrical power and running time for each mode in yearly simulations

| Month | ORC | | HP | | Direct heating |
|-----------|-------------------------|------------------|------------------------------|----------------------|----------------------|
| | Net energy output [kWh] | Running time [h] | Electrical consumption [kWh] | Heating energy [kwh] | Heating energy [kWh] |
| January | - | - | 218.09 | 613.6 (61h) | 515.4 |
| February | 50.8 | 27 | - | - | 1077.6 |
| March | 193.1 | 92 | - | - | 979.2 |
| April | 519.9 | 202 | - | - | 720.5 |
| May | 750.7 | 269 | - | - | 392.3 |
| June | 708.9 | 276 | - | - | 225.3 |
| July | 798.7 | 295 | - | - | 225.3 |
| August | 626.9 | 253 | - | - | 220.2 |
| September | 302.1 | 163 | - | - | 249.5 |
| October | 79.1 | 76 | - | - | 602.4 |
| November | - | - | 3.82 | 12.5 (1h) | 815 |
| December | - | - | 305.4 | 795.6 (89h) | 266.5 |
| Total | 4030.2 | 1653 | 527.3 | 1421.7 | 6289.2 |

4.3 Selection of the fluid

First, R134a has been pre-selected thanks to the Scroll expander operating map (Quoilin 2011). Previous works have examined principal refrigerants appropriate for a low temperature ORC application (Quoilin et al 2011) and suggests those typical fluids: R123, R1234yf, R124, R134a, R152a, R600 and R600a. Each fluid is compared using the yearly simulation and a multi-criteria approach (Quoilin et al 2011). Table 4 shows the annual electrical energy produced and inconvenient for each fluid. Some fluids (R245fa and R123) can be rejected mainly because of the low electrical production. Others presents a significant increase in electrical production (R124, R600, R152a and R600a) but are rejected because of environmental reasons or flammability. The chosen working fluid is thus the R134a although its relatively low performance.

Table 4: Selection of the working fluid

| Fluid | Electrical Production [kWh/year] | GWP [-] | ODP [-] | Inconvenient |
|--------|----------------------------------|---------|---------|-------------------------------------|
| R124 | 5079 | 120 | 0.026 | Environmental reasons |
| R600 | 4239 | 20 | 0 | Flammability |
| R152a | 3969 | 120 | 0 | Flammability |
| R600a | 3814 | 20 | 0 | Flammability |
| R245fa | 3349 | 950 | 0 | Toxicity + low W_{net} |
| R123 | 3105 | 120 | 0.012 | Environment reasons + low W_{net} |
| R134a | 3772 | 1300 | 0 | - |

4.4 Selection of the compressor/expander

The selection of the compressor is done by comparing their electrical production in ORC mode and electrical consumption in HP mode with the refrigerant R134a. Table 5 presents results from yearly simulations with three different compressors with fluid R134a. In ORC mode, compressor B is the best one. This can be explained physically: Too small of a compressor (compressor A for example) leads to a maximum electrical production that limits the performance when large amount of heat are generated in summer. Too large of a compressor leads to low electrical production at part load because it is working mainly at low pressure ratio (zone where the isentropic efficiency is low). In heat pump mode, the same compressor B is the more suited to our application.

Table 5: Selection of the compressor

| Compressor | A | B | C |
|-----------------------------|------|------|------|
| ORC annual production [kWh] | 3834 | 4030 | 3910 |
| HP annual consumption [kWh] | 532 | 527 | 611 |

5 EXPERIMENTATION

5.1 Experimental setup

An experimental study has been carried out on the ORC/HP prototype with refrigerant R134a. Figures 5 presents the detailed scheme of the installation with the refrigerant loop in light blue. The heat source (red) consists of an electrical oil boiler with a maximum output of 150 kW. The condenser is cooled by tap water (light blue).

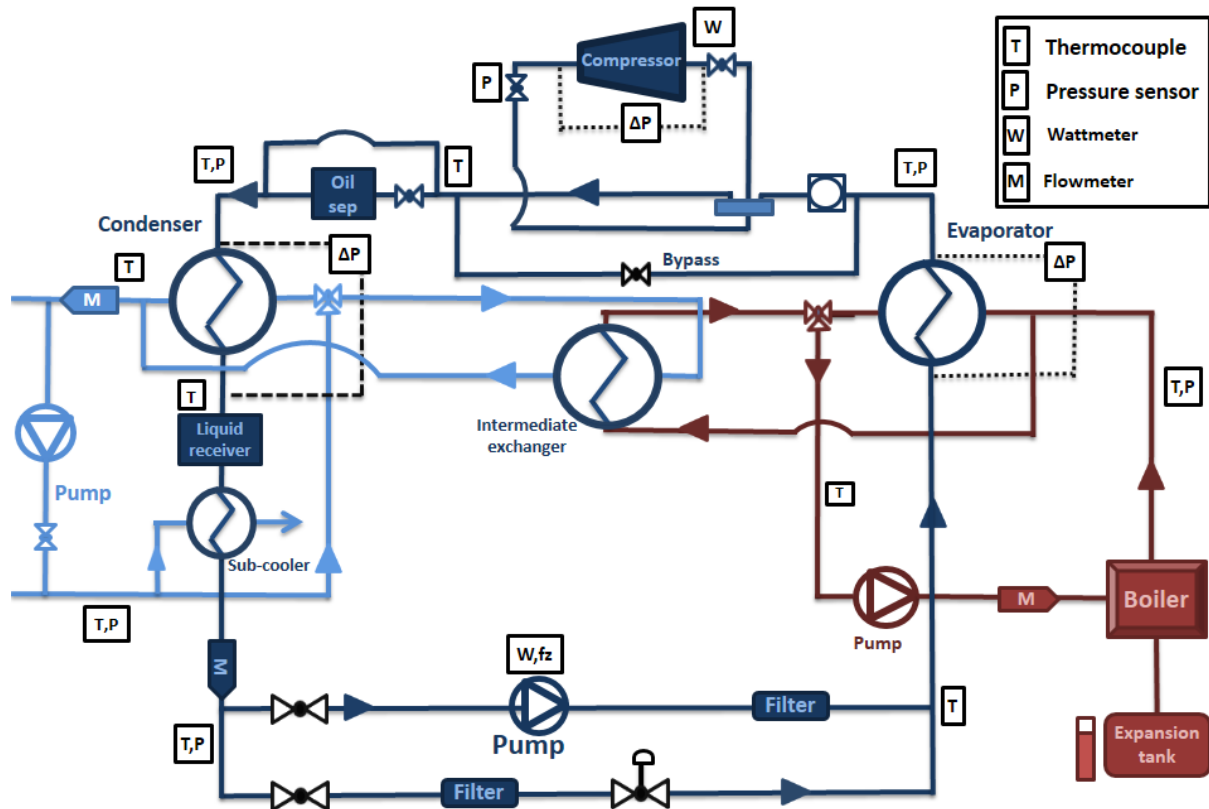


Figure 5: Experimental configuration of the HP/ORC reversible unit

5.2 Experimental results

Experimental results are presented in Table 6. They are compared with theoretical expectations in HP and ORC modes for a similar operating point. First, these results prove the feasibility of such a reversible unit with encouraging performance. However some results are slightly worse than what was expected because of:

- The lower expander isentropic efficiency and high filling factor (i.e. high leakages between high pressure and low pressure).
- The large pressure drop on the four ways valve (up to 4 bars). The four way valve is a component utilized to switch the inlet and outlet of the compressor to commute from one mode to another.
- Necessary sub-cooling to avoid the cavitation of the pump

A higher efficiency of 5.7% is achieved in ORC mode but with lower evaporator power. The efficiency is lower at higher evaporator power because of the high pressure drop on the four ways valve when high flow are needed.

5.3 Improvements

Several improvements are possible:

- Replacing the four ways valve to decrease the pressure drop.
- Controlling the speed of the expander. That will allow to regulate the evaporation temperature and it will therefore allow to optimize the working conditions.
- Developing an expander with an optimized geometry.
- Developing a compressor with a higher maximum admissible pressure (32 bar).
- Using a more efficient pump.

Table 6: Comparison of theoretical and experimental results for two similar operating points (Global efficiency in ORC mode is equal to net electrical production divided by the evaporation heat)

| Mode | Parameter | Nominal theoretical point | Experiment |
|------|-----------------------------|---------------------------|------------|
| ORC | Evaporator power [kW] | 62 | 62 |
| | Evaporation pressure [bar] | 33 | 32 |
| | Condensation pressure [bar] | 7 | 10.3 |
| | Mass flow [g/s] | 300 | 266 |
| | Electrical power [kW] | 4.7 | 3.7 |
| | Global efficiency [%] | 7.5 | 4.2 |
| | Isentropic efficiency [%] | 68 | 58 |
| | Filling factor [-] | 1.019 | 1.12 |
| HP | Condenser power [kW] | 13 | 13.6 |
| | Evaporator pressure [bar] | 5 | 5.7 |
| | Condensation pressure [bar] | 17 | 17.3 |
| | Mass flow [g/s] | 100 | 102 |
| | Electrical power [kW] | 4 | 3.8 |
| | COP [-] | 4.25 | 4.21 |
| | Isentropic efficiency [%] | 60 | 76 |
| | Volumetric efficiency [%] | 91 | 97 |

6 CONCLUSION

This study proposes an innovative reversible domestic HP/ORC system, allowing for both heat and electricity production depending on the weather conditions. A detailed model of the system was built and allowed sizing the components. These simulation also allow us to predict an annual electrical production of 4030 kWh. The electrical consumption in HP mode reach 527.3 kWh over a year. 6289.2 kWh is provided by the direct heating mode. Following that, the technical feasibility of such a reversible unit has been demonstrated. An ORC efficiency of 4.2 is reached and a COP of 4.21 is obtained in conditions comparable to theoretical predictions. Finally, major means to improve the system performance have been pointed out.

After a complete experimental investigation of the unit has been done, the unit is installed and monitored in a house in Herning (Denmark) and some perspectives are listed hereunder:

- Automation of each mode of the unit including control strategies to switch optimally from one mode to another.
- Validation a steady state model of each component and of the global system based on the experimental investigation.
- Evaluation of the performance on yearly simulation based on these experimental validation.
- Creation of a second, more efficient unit.

7 REFERENCES

Delta calor, 2013. "Thermal losses in a storage." http://herve.silve.pagesperso-orange.fr/bilan_th.htm. [accessed January 2014]

European standard European Standards 1999. "Refrigerant compressors - Rating conditions, tolerances and presentation of manufacturer's performance data", DIN EN 12900.

Garcia-Cascales, J.R., Vera-Garcia, F., Corberan-Salvador, J.M., Gonzalez-Macia, J., 2007. "Assessment of boiling and condensation heat transfer correlations in the modelling of plate heat exchangers," *International Journal of Refrigeration*, Vol. 30, pp. 1029-1041.

Hsieh, Y. Y., and Lin, T. F. 2002. "Saturated flow boiling heat transfer and pressure drop of refrigerant R-410A in a vertical plate heat exchanger," *International Journal of Heat and Mass Transfer*, Vol. 45, Part 5, pp. 1033-1044.

Innogie 2013, <http://www.innogie.dk>. [accessed January 2014].

Kuo, W. S., Lie, Y. M., Hsieh, Y. Y., and Lin, T. F. 2005. "Condensation heat transfer and pressure drop of refrigerant R-410A flow in a vertical plate heat exchanger," *International Journal of Heat and Mass Transfer*, Vol. 48, Part 25-26, pp. 5205-5220.

Lemort, V. 2008. "Contribution to the characterization of Scroll machine in compressor and expander modes," PhD. Thesis, University of Liege, Liege.

Lemort, V., Quoilin, S., Cuevas, C., and Lebrun, J. 2009. "Testing and modeling a scroll expander integrated into an Organic Rankine Cycle," *Applied Thermal Engineering*, Vol 29, Part 14–15, pp. 3094-3102.

Lemort, V., Declaye, S., and Quoilin, S., 2011. "Experimental characterization of a hermetic scroll expander for use in a micro-scale Rankine cycle," *Journal of Power and Energy*, Vol. 0, part 0, pp. 1-10.

Pérez-Lombard, L., Ortiz, J., Pout, C. 2008. "A review on buildings energy consumption information," *Energy and building*, Vol. 40, pp. 394-398.

Quoilin, S., 2011. "Sustainable Energy Conversion Through the use of Organic Rankine Cycles for Waste Heat Recovery and Solar Applications," Ph.D. thesis, University of Liege, Liege.

Quoilin, S., Declaye, S., Tchanche, B.F., Lemort, V. 2011. "Thermo-economic optimization of waste heat recovery Organic Rankine Cycles," *Applied Thermal Engineering*, Vol. 31, pp. 2885-2893.

Schimpf, S., Span, R. (2013) "Combining a thermally supported ground source heat pump with an ORC process." Draft for an oral session at the 2nd ORC conference 2013.

Thonon B., 1995. "Recent research and developments in plate heat exchangers," *Fuel and Energy Abstracts*, Vol. 36, Part 5, pp. 361.

DESIGN, MODELLING, PERFORMANCE OPTIMIZATION AND EXPERIMENTATION OF A REVERSIBLE HP/ORC PROTOTYPE

*Olivier, Dumont, PhD student, Thermodynamics and Energetics Laboratory
Chemin des chevreuils, 7 (B49), 4000 Liege, Belgium*

*Sylvain, Quoilin, Post-doctoral research associate, Thermodynamics and Energetics
Laboratory Chemin des chevreuils, 7 (B49), 4000 Liege, Belgium*

*Vincent, Lemort, Professor, Thermodynamics and Energetics Laboratory
Chemin des chevreuils, 7 (B49), 4000 Liege, Belgium*

Abstract: This paper presents an innovative system comprising a water/water heat pump connected to a solar roof and a geothermal heat exchanger. This unit is able to invert its cycle and operate as an Organic Rankine Cycle. The solar roof is producing a large amount of heat throughout the year. This allows covering the building annual heating needs and furthermore, electricity is produced thanks to the surplus of heat in a so-called HP/ORC reversible unit. This paper is focusing on these three main points: modeling, design and experimentation of the prototype. This paper demonstrates the feasibility of such a prototype with encouraging performance in ORC and HP modes. First simulations of the HP/ORC system, with components optimally sized, indicate that, in ORC mode, for the weather conditions of Copenhagen, the electrical energy produced over one year reaches 4030 kWh and the nominal efficiency of the cycle is 7.6%. The nominal COP of the heat pump is 4.2 (condenser exhaust temperature of 60°C and evaporator supply temperature of 15°C). Experimentally, a COP of 4.21 (condensation temperature of 61°C and evaporation temperature of 21°C) is achieved in heat pump mode and a global ORC efficiency of 5.7% is obtained in ORC mode (condenser exhaust temperature of 25°C and evaporator supply temperature of 88°C)..

Key Words: Heat pump, ORC, modeling, Scroll compressor, reversible

1 INTRODUCTION

A important sector where measures must be adopted to significantly reduce energy consumption and greenhouse gases emissions is the building sector (37% of the total final energy consumption of the EU (Perez et al 2008)). In this context, heat pumps provides energy-efficient space and domestic hot water heating in many applications (Hepbasli 2009, Georges 2013). This paper presents an innovative system comprising a water/water heat pump connected to a solar roof and a geothermal heat exchanger (Figure 1). This heat pump is reversible, meaning that it can be run as an Organic Rankine Cycle (ORC). A large amount of heat (sometimes more than 100 kW) is generated throughout the year by the solar roof. This heat is used in priority to cover the building heating needs and the surplus heat generated is utilized in a so-called HP/ORC module to generate electricity. It also works as an efficient heat pump which simplifies the complexity of the total system compared to competitive products (heat pump combined with photovoltaics for example).

There is only one reference exploring this concept in literature (Schimpf 2013). It focuses on yearly simulation and thermo-economic feasibility of the system in a classical house with

accurate models for solar collectors, heat storage and ground heat exchanger. The concept presented in this paper is different from Schimpf's work because the house (ground heat exchanger and solar absorber) is built around the module for a better integration. This leads to a larger solar roof (15 times larger) and a longer ground heat exchanger that allows to produce much more electricity through the year. The prototype is already built and installed in the house in Herring (Denmark) and is working nowadays (Innogie 2013).

This paper is organized as follows: First a short description of the concept with the three different operating modes is done. After that, the modeling of each component is detailed and a complete sizing model is developed. This model is used to assess the performance of the system in both ORC and HP modes. Finally, results from experimentation are described.

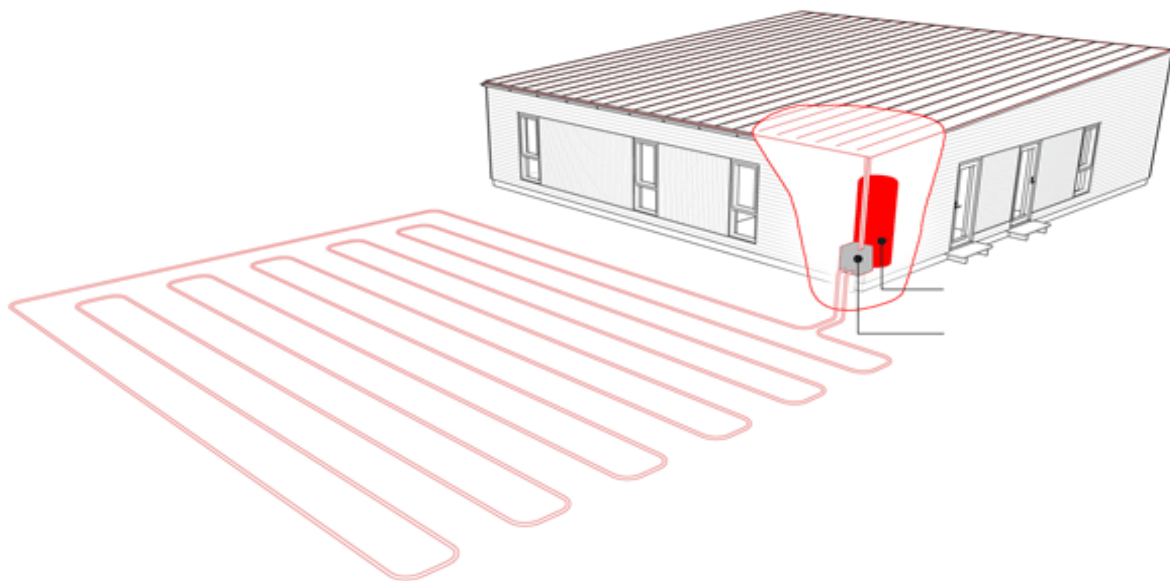


Figure 1: The reversible HP/ORC unit integrated into the house with a solar absorber and the ground heat exchanger (Innogie 2013)

2 WORKING PRINCIPLE

2.1.1 Organic Rankine Cycle mode

When the heating requirements of the house are covered by the heat storage and that the weather conditions are appropriate, the ORC mode is used to generate electricity (Figure 2). The working process is relatively simple: heat coming from the roof evaporates the working fluid through the evaporator. Then, the working fluid expands in the scroll device generating electricity. Following this, the refrigerant (R134a) is condensed thanks to the ground heat exchanger and goes into the pump before starting the cycle again.

2.1.2 Heat Pump mode

When heating requirements of the house cannot be covered by the heat storage or by the direct heating mode, the heat pump mode is activated. The components necessary to use the heat pump are almost the same as the ORC mode except that the pump is bypassed by an electronic expansion valve and that the condenser is connected to the heat storage. It works as a classical water to water heat pump, with its evaporator connected to the solar roof.

2.1.3 Direct heating mode

This mode is used as long as the heat storage cannot cover the heat requirements and provided that the heat transfer rate exchanged with the roof is sufficient. The heat goes from the solar absorber to the heat storage through a heat exchanger.

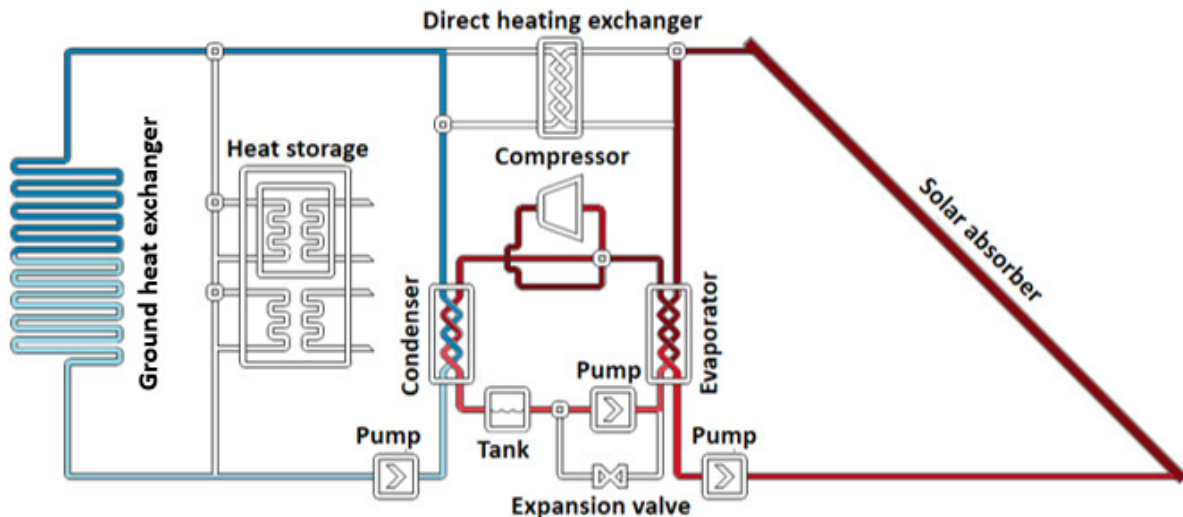


Figure 2: Reversible HP/ORC detailed scheme (ORC mode)

3 MODELLING

3.1 Compressor - expander

The machine used as an expander or as a compressor following the operating mode is a modified scroll compressor. This choice has been based on the ability of this machine to work in both mode and because this is the more efficient expansion device for low power (<10kWel) solar applications (Quoilin 2011). The compressor is simulated by empirical correlation from the manufacturer (Emerson 2013) following European standard (European standard 1999). There are no efficiency data available for the expander mode from the manufacturer. A semi-empirical model, proposed by (Lemort 2008) and validated by tests with R245fa (Lemort et al 2011) is used. The model requires only nine parameters (heat transfer coefficients, friction torque, leakage area and pressure drop equivalent diameter). They are scaled with the laws proposed by (Lemort 2008).

3.2 Exchangers

Plate heat exchangers are chosen for the condenser, evaporator and direct heating exchanger because they present good efficiencies, compactness's and prices. A three zones model is considered. Heat transfer coefficients are evaluated with Thonon's correlation for single phase zones (Thonon 1995), with Kuo's correlation for condensation (Kuo 2005) and with Hsieh's correlation for evaporation (Hsieh 2002). These models are validated with R410 and are used for R134a in this paper because models for plate heat exchangers are very scarce and because results diverge from one to another (Garcia-Cascales, 2007). In the sizing model, the surface and the number of plates are evaluated trough an imposed pinch-point and a maximum pressure drop on refrigerant side (Quoilin 2011). The surface and the number of plates are of course imposed in the simulation model.

3.3 Solar roof

The roof is modeled by a simple linear model (Innogie 2013) because this work is more focused on the HP/ORC unit. S_{abs} is the total absorber area (150 m²), $\eta_{glazing}$ is the optical efficiency, i.e. the transmissivity, (88%), T_{amb} is the ambient temperature, I is the current solar insolation (in W/m²) and ΔT_{abs} is the difference between the ambient temperature and the average heat transfer fluid temperature in the collector.

$$\dot{Q}_{abs} [W] = S_{abs} (-26.2 - 1.22T_{amb} - 1.7 \Delta T_{abs} + 0.903 I) \quad (1)$$

$$\eta_{abs} [-] = \frac{\dot{Q}_{abs} \cdot \eta_{glazing}}{I \cdot S_{abs}} \quad (2)$$

3.4 Storage

A model of storage including ambient losses (Q_{sto}) is used (Delta calor, 2013). The volume (V_{sto}) and the storage temperature (T_{sto}) are imposed at 1000 litres and 55°C respectively.

$$Q_{sto} \left[\frac{Wh}{day} \right] = 4,2 \cdot V_{sto}^{0,47} \cdot (T_{sto} - T_{amb}) \quad (3)$$

3.5 Pump

Constraints on the flow in ORC mode - relatively high pressure drops (≈ 20 bar) and low flow (≈ 300 g/s) – leads to the use of a volumetric pump. A plunger pump is chosen based on its efficiency, price and tightness. The pump is modeled with a constant isentropic efficiency (ϵ_{is}) of 0.5 (Equation 5). This allows to evaluate the electrical consumption of the pump (\dot{W}_{pp}). \dot{m} is the mass flow, $h_{ex,is}$ is the isentropic enthalpy at the exhaust of the pump and h_{su} is the supply enthalpy of the pump.

$$\epsilon_{is} [-] = \frac{\dot{m} (h_{ex,is} - h_{su})}{\dot{W}_{pp}} \quad (5)$$

4 SIZING

4.1 Definition of the nominal conditions

Since all the components models are detailed, nominal conditions are necessary to size our components. The ORC mode is the one involving the highest heat flow exchanged with the heat source and sink, it is therefore the one selected for the sizing of the system components.

The nominal sizing conditions are defined as follows:

- The evaporating temperature is set to 90°C, which approximately corresponds to the maximum pressure at the inlet of the expander (32 bars) with the selected fluid.
- On the cooling water side, an inlet temperature of 15°C and an outlet temperature of 20°C are assumed.
- The heat source temperature glide, i.e. the difference between the inlet and outlet glycol water temperature on the absorber, is set to 25K in order to conserve a reasonable glycol water flow rate.
- The pinch points are set to 5K for the evaporator and 7.5K for the condenser (Quoilin et al 2011).

- The superheating and sub-cooling of the evaporator and the condenser are set to 10K and 2K respectively.

For the heat pump mode, the following operating conditions are imposed:

- The evaporating temperature (15,7°C) is selected as the equilibrium temperature when the heat pump heating capacity is 8 kWth and when the solar radiation is 90 W/m². This is representative of winter conditions in Denmark.

- The glycol water flow rate (evaporator) is set to the value provided by the ORC mode, depending on the scroll machine power.

- The condensing temperature is fixed to 60°C in order to get a water temperature around 55°C at the inlet of the heat storage (value chosen to be conservative). This temperature is sufficient to cover all the needs of the house.

- For hot water production, a temperature difference of 5K is assumed between the inlet and the outlet of the condenser.

- The superheating and sub-cooling of the evaporator and the condenser are set to 3K and 2K respectively.

The heat exchangers and the pump are sized using the nominal summer conditions. However, the size of the scroll machine (which defines the net power of the system, both in HP and ORC mode) results from a tradeoff between winter and summer performance. This can only be optimized using yearly simulations, as proposed in the section 4.2. The results presented in Table 1 for the nominal conditions have been obtained with the optimal expander size (swept volume = 98.04 cm³) and the optimal fluid (R134a) resulting from yearly simulation optimization (see section 4.2).

Table 1: Nominal conditions

| Mode | Parameter | Value |
|-----------|--------------------------------------|-------|
| Heat pump | Evaporation pressure [bar] | 5 |
| | Condensation pressure [bar] | 17 |
| | Power consumed [W] | 3211 |
| | Mass flow[kg/s] | 0.1 |
| | Compressor isentropic efficiency [%] | 60 |
| | Absorber efficiency [%] | 56 |
| | COP [-] | 4.2 |
| ORC | Evaporation pressure [bar] | 33 |
| | Condensation pressure [bar] | 7 |
| | Power produced [W] | 4733 |
| | Mass flow[kg/s] | 0.3 |
| | Expander isentropic efficiency [%] | 68 |
| | Absorber efficiency [%] | 55 |
| | ORC global efficiency [%] | 7.6 |

4.2 Yearly simulations

In the previous section, the performance of the system has been evaluated on a nominal sizing point, allowing to select and to define the geometry of some components. However when optimizing the design, it is important to account for the performance of the system over a whole year. The system is therefore simulated over a whole year (with one hour time step) by taking into account the average climatic conditions, the average building heat demand for each month of the year and the control strategy. The outside temperature and the solar irradiance are inputs based on Copenhagen since the unit is installed in Denmark. The following control strategy is used: The ORC mode is used as long as the heat storage can

cover the heat demand. If this is not the case, the direct heating mode is activated. Finally, the HP mode is selected for severe climate conditions when the direct heating mode does not allow reaching the required heating temperature.

These simulations allow optimizing discrete variables such as the choice of the working fluid, the use of a recuperator, and the size of the scroll machine (available sizes are taken from the catalog of one manufacturer). The following methodology is applied:

1. For a given configuration (fluid, expander size, recuperator or not), the condenser and of the evaporator are re-sized in term of area and number of plates and the system performance is evaluated over a wide range of evaporation/condensation temperatures, both for the ORC mode and the HP mode. This is done with the nominal condition methodology (see section 4.1).
2. Performance curves are derived from these simulations as a function of the system configuration and of the temperature levels.
3. These curves are implemented in the yearly simulation model, which optimally switches between the three operating modes depending on the weather conditions and on the heat demand.

Point 2 is achieved by running the simulation model for different mean absorber temperatures in order to see the evolution of the electrical power and the heat transfer to the evaporator. In this example, the performance of three compressors (A, B and C) are compared. Technical data is presented in Table 2. This curves are shown for the ORC mode (Figure 3) and for the HP mode (Figure 4).

Table 2: Technical data of the three compressors

| Compressor Parameter | Case A | Case B | Case C |
|------------------------|--------|--------|--------|
| Swept volume [-] | 82.6 | 98.04 | 119.96 |
| Volume ratio [-] | ≈ 3 | ≈ 3 | ≈ 3 |
| Maximum pressure [bar] | 32 | 32 | 32 |

For the ORC mode, the power transferred (\dot{Q}_{ev} continuous line – Figure 3) increases when the mean absorber temperature (\bar{T}) rises and thus net output power (\dot{W}_{net}) increases too. This is due to the fact that the evaporating temperature and pressure increase when the hot source temperature rises, hot source flow rate being constant. However it is important not to exceed the maximum pressure at the expander inlet. This involves a limitation on the power generation. Though, in order to increase the electrical power when the maximum pressure is reached, the pressure is fixed at its maximum value and the super-heating is increased. This explains the discontinuity appearing around 95°C. It can be seen that when the maximum pressure is reached, increasing the superheating involves a decrease in the thermal power transferred (continuous lines) but it allows increasing still a bit more the power produced (dashed lines). From these curves, polynomial laws have been fitted in order to perform the yearly simulation:

$$\dot{Q}_{ev} = C_0 + C_1 \cdot \bar{T} + C_2 \cdot \bar{T}^2 \quad (6)$$

$$\dot{W}_{net} = K_0 + K_1 \cdot \bar{T} + K_2 \cdot \bar{T}^2 \quad (7)$$

For the next step, in the yearly simulation, the mean glycol water temperature will be computed from the weather data (ambient temperature and solar radiation) and from the polynomial expression of the thermal power transferred (Equation 8). This will therefore allow determining the mean absorber temperature corresponding to the weather data and then, the related power generation and the performance of the system in the ORC mode.

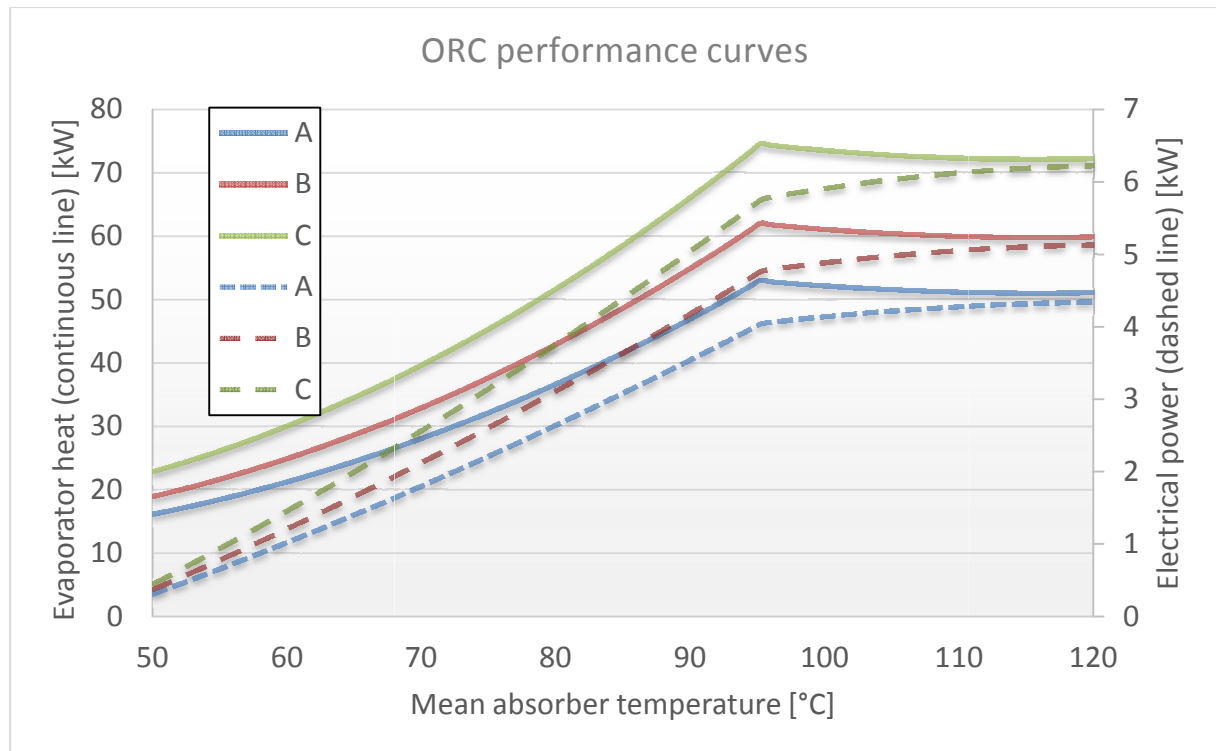


Figure 3: ORC performance curves in function of the mean absorber temperature

In heat pump mode, the sizing of the exchangers is the same as in ORC mode because the thermal power is higher. The simulation model has been run for different mean absorber temperatures in order to see the evolution of the electrical power consumption with the thermal power transferred to the evaporator and operating conditions (Figure 4). The thermal power transferred to the evaporator () and the electrical power consumption () increases when the mean absorber temperature rises. The thermal power recovered at the condenser () increases therefore too because the energy balance on the heat pump gives:

$$(8)$$

Moreover, as the ORC mode, polynomial laws have been derived from these curves for yearly simulations. The weather conditions combined with these polynomial expressions will allow us to determine the mean absorber temperature, the thermal power recovered at the condenser and the performance of the heat pump.

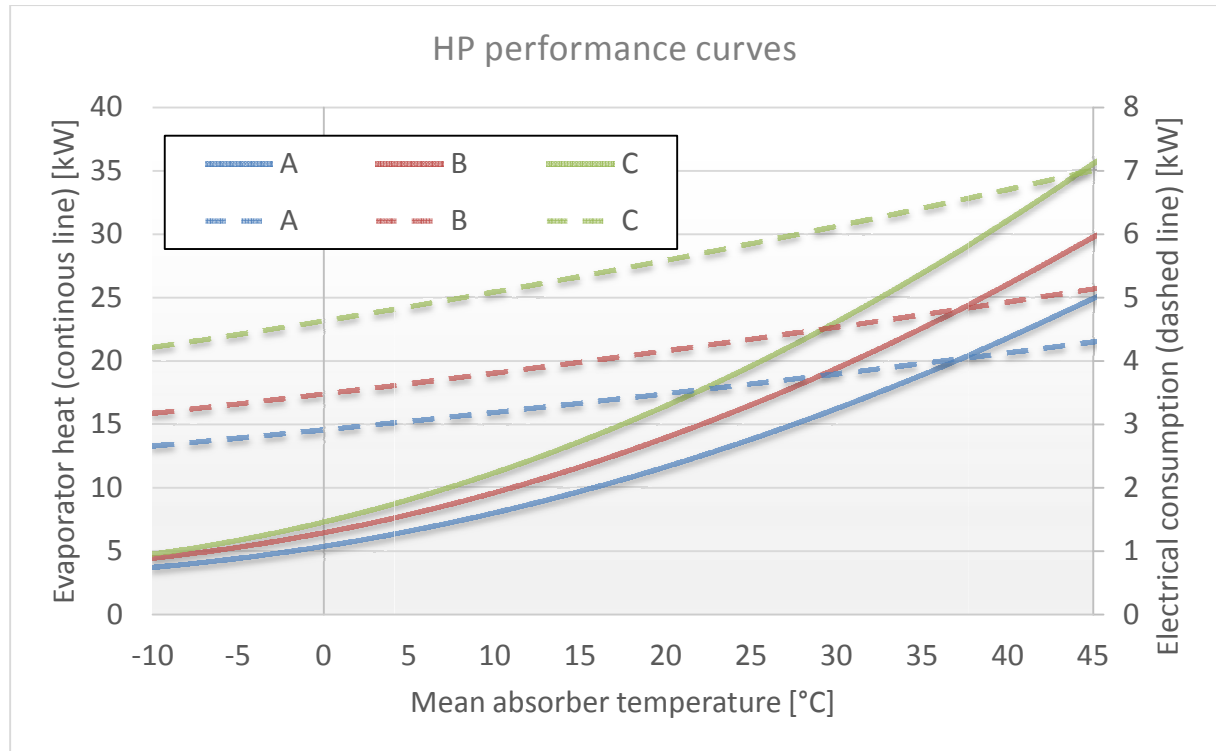


Figure 4: HP performance curves in function of the mean absorber temperature

Finally, the addition of the heat demand of the house and the thermal losses of the heat storage gives the total energy that the unit needs to produce.

Table 3 presents the results in terms of electrical power and running time from these yearly simulation in the case of compressor B and with the optimum fluid (see section 4.3). The heat pump mode is only used during 3 months. The rest of the year, the direct heating is sufficient to provide the heat required by the building and the ORC mode allows producing electricity with the surplus heat.

Table 3: Electrical power and running time for each mode in yearly simulations

| Month | ORC | | HP | | Direct heating |
|-----------|-------------------------|------------------|------------------------------|----------------------|----------------------|
| | Net energy output [kWh] | Running time [h] | Electrical consumption [kWh] | Heating energy [kwh] | Heating energy [kWh] |
| January | - | - | 218.09 | 613.6 (61h) | 515.4 |
| February | 50.8 | 27 | - | - | 1077.6 |
| March | 193.1 | 92 | - | - | 979.2 |
| April | 519.9 | 202 | - | - | 720.5 |
| May | 750.7 | 269 | - | - | 392.3 |
| June | 708.9 | 276 | - | - | 225.3 |
| July | 798.7 | 295 | - | - | 225.3 |
| August | 626.9 | 253 | - | - | 220.2 |
| September | 302.1 | 163 | - | - | 249.5 |
| October | 79.1 | 76 | - | - | 602.4 |
| November | - | - | 3.82 | 12.5 (1h) | 815 |
| December | - | - | 305.4 | 795.6 (89h) | 266.5 |
| Total | 4030.2 | 1653 | 527.3 | 1421.7 | 6289.2 |

4.3 Selection of the fluid

First, R134a has been pre-selected thanks to the Scroll expander operating map (Quoilin 2011). Previous works have examined principal refrigerants appropriate for a low temperature ORC application (Quoilin et al 2011) and suggests those typical fluids: R123, R1234yf, R124, R134a, R152a, R600 and R600a. Each fluid is compared using the yearly simulation and a multi-criteria approach (Quoilin et al 2011). Table 4 shows the annual electrical energy produced and inconvenient for each fluid. Some fluids (R245fa and R123) can be rejected mainly because of the low electrical production. Others presents a significant increase in electrical production (R124, R600, R152a and R600a) but are rejected because of environmental reasons or flammability. The chosen working fluid is thus the R134a although its relatively low performance.

Table 4: Selection of the working fluid

| Fluid | Electrical Production [kWh/year] | GWP [-] | ODP [-] | Inconvenient |
|--------|----------------------------------|---------|---------|-------------------------------------|
| R124 | 5079 | 120 | 0.026 | Environmental reasons |
| R600 | 4239 | 20 | 0 | Flammability |
| R152a | 3969 | 120 | 0 | Flammability |
| R600a | 3814 | 20 | 0 | Flammability |
| R245fa | 3349 | 950 | 0 | Toxicity + low W_{net} |
| R123 | 3105 | 120 | 0.012 | Environment reasons + low W_{net} |
| R134a | 3772 | 1300 | 0 | - |

4.4 Selection of the compressor/expander

The selection of the compressor is done by comparing their electrical production in ORC mode and electrical consumption in HP mode with the refrigerant R134a. Table 5 presents results from yearly simulations with three different compressors with fluid R134a. In ORC mode, compressor B is the best one. This can be explained physically: Too small of a compressor (compressor A for example) leads to a maximum electrical production that limits the performance when large amount of heat are generated in summer. Too large of a compressor leads to low electrical production at part load because it is working mainly at low pressure ratio (zone where the isentropic efficiency is low). In heat pump mode, the same compressor B is the more suited to our application.

Table 5: Selection of the compressor

| Compressor | A | B | C |
|-----------------------------|------|------|------|
| ORC annual production [kWh] | 3834 | 4030 | 3910 |
| HP annual consumption [kWh] | 532 | 527 | 611 |

5 EXPERIMENTATION

5.1 Experimental setup

An experimental study has been carried out on the ORC/HP prototype with refrigerant R134a. Figures 5 presents the detailed scheme of the installation with the refrigerant loop in light blue. The heat source (red) consists of an electrical oil boiler with a maximum output of 150 kW. The condenser is cooled by tap water (light blue).

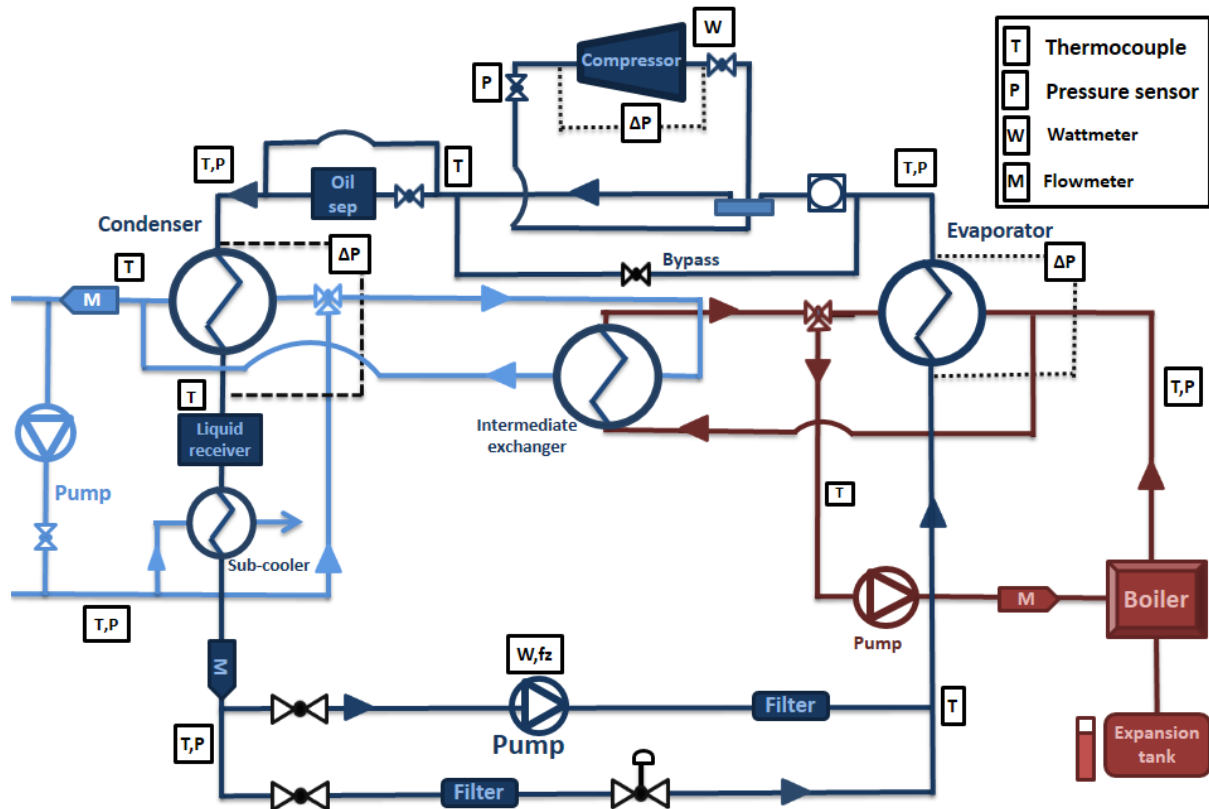


Figure 5: Experimental configuration of the HP/ORC reversible unit

5.2 Experimental results

Experimental results are presented in Table 6. They are compared with theoretical expectations in HP and ORC modes for a similar operating point. First, these results prove the feasibility of such a reversible unit with encouraging performance. However some results are slightly worse than what was expected because of:

- The lower expander isentropic efficiency and high filling factor (i.e. high leakages between high pressure and low pressure).
- The large pressure drop on the four ways valve (up to 4 bars). The four way valve is a component utilized to switch the inlet and outlet of the compressor to commute from one mode to another.
- Necessary sub-cooling to avoid the cavitation of the pump

A higher efficiency of 5.7% is achieved in ORC mode but with lower evaporator power. The efficiency is lower at higher evaporator power because of the high pressure drop on the four ways valve when high flow are needed.

5.3 Improvements

Several improvements are possible:

- Replacing the four ways valve to decrease the pressure drop.
- Controlling the speed of the expander. That will allow to regulate the evaporation temperature and it will therefore allow to optimize the working conditions.
- Developing an expander with an optimized geometry.
- Developing a compressor with a higher maximum admissible pressure (32 bar).
- Using a more efficient pump.

Table 6: Comparison of theoretical and experimental results for two similar operating points (Global efficiency in ORC mode is equal to net electrical production divided by the evaporation heat)

| Mode | Parameter | Nominal theoretical point | Experiment |
|------|-----------------------------|---------------------------|------------|
| ORC | Evaporator power [kW] | 62 | 62 |
| | Evaporation pressure [bar] | 33 | 32 |
| | Condensation pressure [bar] | 7 | 10.3 |
| | Mass flow [g/s] | 300 | 266 |
| | Electrical power [kW] | 4.7 | 3.7 |
| | Global efficiency [%] | 7.5 | 4.2 |
| | Isentropic efficiency [%] | 68 | 58 |
| | Filling factor [-] | 1.019 | 1.12 |
| HP | Condenser power [kW] | 13 | 13.6 |
| | Evaporator pressure [bar] | 5 | 5.7 |
| | Condensation pressure [bar] | 17 | 17.3 |
| | Mass flow [g/s] | 100 | 102 |
| | Electrical power [kW] | 4 | 3.8 |
| | COP [-] | 4.25 | 4.21 |
| | Isentropic efficiency [%] | 60 | 76 |
| | Volumetric efficiency [%] | 91 | 97 |

6 CONCLUSION

This study proposes an innovative reversible domestic HP/ORC system, allowing for both heat and electricity production depending on the weather conditions. A detailed model of the system was built and allowed sizing the components. These simulation also allow us to predict an annual electrical production of 4030 kWh. The electrical consumption in HP mode reach 527.3 kWh over a year. 6289.2 kWh is provided by the direct heating mode. Following that, the technical feasibility of such a reversible unit has been demonstrated. An ORC efficiency of 4.2 is reached and a COP of 4.21 is obtained in conditions comparable to theoretical predictions. Finally, major means to improve the system performance have been pointed out.

After a complete experimental investigation of the unit has been done, the unit is installed and monitored in a house in Herning (Denmark) and some perspectives are listed hereunder:

- Automation of each mode of the unit including control strategies to switch optimally from one mode to another.
- Validation a steady state model of each component and of the global system based on the experimental investigation.
- Evaluation of the performance on yearly simulation based on these experimental validation.
- Creation of a second, more efficient unit.

7 REFERENCES

Delta calor, 2013. "Thermal losses in a storage." http://herve.silve.pagesperso-orange.fr/bilan_th.htm. [accessed January 2014]

European standard European Standards 1999. "Refrigerant compressors - Rating conditions, tolerances and presentation of manufacturer's performance data", DIN EN 12900.

Garcia-Cascales, J.R., Vera-Garcia, F., Corberan-Salvador, J.M., Gonzalez-Macia, J., 2007. "Assessment of boiling and condensation heat transfer correlations in the modelling of plate heat exchangers," *International Journal of Refrigeration*, Vol. 30, pp. 1029-1041.

Hsieh, Y. Y., and Lin, T. F. 2002. "Saturated flow boiling heat transfer and pressure drop of refrigerant R-410A in a vertical plate heat exchanger," *International Journal of Heat and Mass Transfer*, Vol. 45, Part 5, pp. 1033-1044.

Innogie 2013, <http://www.innogie.dk>. [accessed January 2014].

Kuo, W. S., Lie, Y. M., Hsieh, Y. Y., and Lin, T. F. 2005. "Condensation heat transfer and pressure drop of refrigerant R-410A flow in a vertical plate heat exchanger," *International Journal of Heat and Mass Transfer*, Vol. 48, Part 25-26, pp. 5205-5220.

Lemort, V. 2008. "Contribution to the characterization of Scroll machine in compressor and expander modes," PhD. Thesis, University of Liege, Liege.

Lemort, V., Quoilin, S., Cuevas, C., and Lebrun, J. 2009. "Testing and modeling a scroll expander integrated into an Organic Rankine Cycle," *Applied Thermal Engineering*, Vol 29, Part 14–15, pp. 3094-3102.

Lemort, V., Declaye, S., and Quoilin, S., 2011. "Experimental characterization of a hermetic scroll expander for use in a micro-scale Rankine cycle," *Journal of Power and Energy*, Vol. 0, part 0, pp. 1-10.

Pérez-Lombard, L., Ortiz, J., Pout, C. 2008. "A review on buildings energy consumption information," *Energy and building*, Vol. 40, pp. 394-398.

Quoilin, S., 2011. "Sustainable Energy Conversion Through the use of Organic Rankine Cycles for Waste Heat Recovery and Solar Applications," Ph.D. thesis, University of Liege, Liege.

Quoilin, S., Declaye, S., Tchanche, B.F., Lemort, V. 2011. "Thermo-economic optimization of waste heat recovery Organic Rankine Cycles," *Applied Thermal Engineering*, Vol. 31, pp. 2885-2893.

Schimpf, S., Span, R. (2013) "Combining a thermally supported ground source heat pump with an ORC process." Draft for an oral session at the 2nd ORC conference 2013.

Thonon B., 1995. "Recent research and developments in plate heat exchangers," *Fuel and Energy Abstracts*, Vol. 36, Part 5, pp. 361.

DESIGN, MODELLING, PERFORMANCE OPTIMIZATION AND EXPERIMENTATION OF A REVERSIBLE HP/ORC PROTOTYPE

*Olivier, Dumont, PhD student, Thermodynamics and Energetics Laboratory
Chemin des chevreuils, 7 (B49), 4000 Liege, Belgium*

*Sylvain, Quoilin, Post-doctoral research associate, Thermodynamics and Energetics
Laboratory Chemin des chevreuils, 7 (B49), 4000 Liege, Belgium*

*Vincent, Lemort, Professor, Thermodynamics and Energetics Laboratory
Chemin des chevreuils, 7 (B49), 4000 Liege, Belgium*

Abstract: This paper presents an innovative system comprising a water/water heat pump connected to a solar roof and a geothermal heat exchanger. This unit is able to invert its cycle and operate as an Organic Rankine Cycle. The solar roof is producing a large amount of heat throughout the year. This allows covering the building annual heating needs and furthermore, electricity is produced thanks to the surplus of heat in a so-called HP/ORC reversible unit. This paper is focusing on these three main points: modeling, design and experimentation of the prototype. This paper demonstrates the feasibility of such a prototype with encouraging performance in ORC and HP modes. First simulations of the HP/ORC system, with components optimally sized, indicate that, in ORC mode, for the weather conditions of Copenhagen, the electrical energy produced over one year reaches 4030 kWh and the nominal efficiency of the cycle is 7.6%. The nominal COP of the heat pump is 4.2 (condenser exhaust temperature of 60°C and evaporator supply temperature of 15°C). Experimentally, a COP of 4.21 (condensation temperature of 61°C and evaporation temperature of 21°C) is achieved in heat pump mode and a global ORC efficiency of 5.7% is obtained in ORC mode (condenser exhaust temperature of 25°C and evaporator supply temperature of 88°C)..

Key Words: Heat pump, ORC, modeling, Scroll compressor, reversible

1 INTRODUCTION

A important sector where measures must be adopted to significantly reduce energy consumption and greenhouse gases emissions is the building sector (37% of the total final energy consumption of the EU (Perez et al 2008)). In this context, heat pumps provides energy-efficient space and domestic hot water heating in many applications (Hepbasli 2009, Georges 2013). This paper presents an innovative system comprising a water/water heat pump connected to a solar roof and a geothermal heat exchanger (Figure 1). This heat pump is reversible, meaning that it can be run as an Organic Rankine Cycle (ORC). A large amount of heat (sometimes more than 100 kW) is generated throughout the year by the solar roof. This heat is used in priority to cover the building heating needs and the surplus heat generated is utilized in a so-called HP/ORC module to generate electricity. It also works as an efficient heat pump which simplifies the complexity of the total system compared to competitive products (heat pump combined with photovoltaics for example).

There is only one reference exploring this concept in literature (Schimpf 2013). It focuses on yearly simulation and thermo-economic feasibility of the system in a classical house with

accurate models for solar collectors, heat storage and ground heat exchanger. The concept presented in this paper is different from Schimpf's work because the house (ground heat exchanger and solar absorber) is built around the module for a better integration. This leads to a larger solar roof (15 times larger) and a longer ground heat exchanger that allows to produce much more electricity through the year. The prototype is already built and installed in the house in Herring (Denmark) and is working nowadays (Innogie 2013).

This paper is organized as follows: First a short description of the concept with the three different operating modes is done. After that, the modeling of each component is detailed and a complete sizing model is developed. This model is used to assess the performance of the system in both ORC and HP modes. Finally, results from experimentation are described.

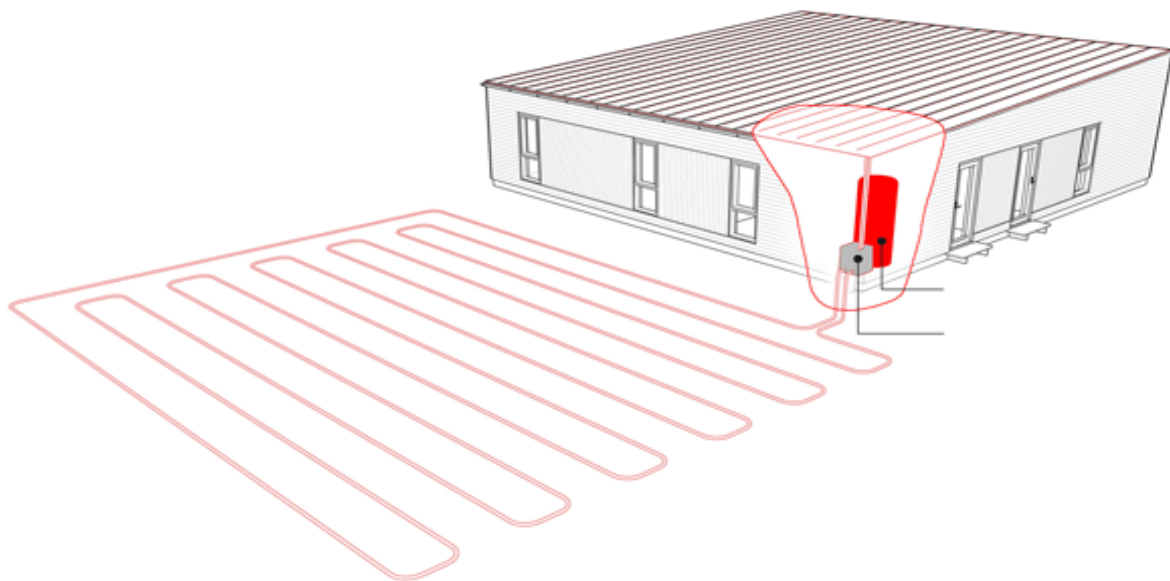


Figure 1: The reversible HP/ORC unit integrated into the house with a solar absorber and the ground heat exchanger (Innogie 2013)

2 WORKING PRINCIPLE

2.1.1 Organic Rankine Cycle mode

When the heating requirements of the house are covered by the heat storage and that the weather conditions are appropriate, the ORC mode is used to generate electricity (Figure 2). The working process is relatively simple: heat coming from the roof evaporates the working fluid through the evaporator. Then, the working fluid expands in the scroll device generating electricity. Following this, the refrigerant (R134a) is condensed thanks to the ground heat exchanger and goes into the pump before starting the cycle again.

2.1.2 Heat Pump mode

When heating requirements of the house cannot be covered by the heat storage or by the direct heating mode, the heat pump mode is activated. The components necessary to use the heat pump are almost the same as the ORC mode except that the pump is bypassed by an electronic expansion valve and that the condenser is connected to the heat storage. It works as a classical water to water heat pump, with its evaporator connected to the solar roof.

2.1.3 Direct heating mode

This mode is used as long as the heat storage cannot cover the heat requirements and provided that the heat transfer rate exchanged with the roof is sufficient. The heat goes from the solar absorber to the heat storage through a heat exchanger.

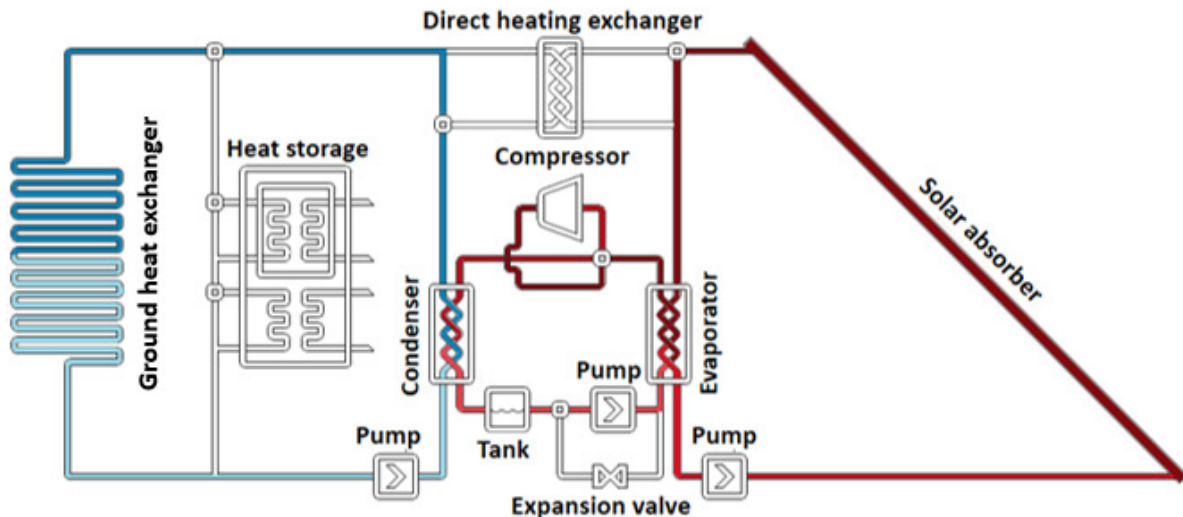


Figure 2: Reversible HP/ORC detailed scheme (ORC mode)

3 MODELLING

3.1 Compressor - expander

The machine used as an expander or as a compressor following the operating mode is a modified scroll compressor. This choice has been based on the ability of this machine to work in both mode and because this is the more efficient expansion device for low power (<10kWel) solar applications (Quoilin 2011). The compressor is simulated by empirical correlation from the manufacturer (Emerson 2013) following European standard (European standard 1999). There are no efficiency data available for the expander mode from the manufacturer. A semi-empirical model, proposed by (Lemort 2008) and validated by tests with R245fa (Lemort et al 2011) is used. The model requires only nine parameters (heat transfer coefficients, friction torque, leakage area and pressure drop equivalent diameter). They are scaled with the laws proposed by (Lemort 2008).

3.2 Exchangers

Plate heat exchangers are chosen for the condenser, evaporator and direct heating exchanger because they present good efficiencies, compactness's and prices. A three zones model is considered. Heat transfer coefficients are evaluated with Thonon's correlation for single phase zones (Thonon 1995), with Kuo's correlation for condensation (Kuo 2005) and with Hsieh's correlation for evaporation (Hsieh 2002). These models are validated with R410 and are used for R134a in this paper because models for plate heat exchangers are very scarce and because results diverge from one to another (Garcia-Cascales, 2007). In the sizing model, the surface and the number of plates are evaluated trough an imposed pinch-point and a maximum pressure drop on refrigerant side (Quoilin 2011). The surface and the number of plates are of course imposed in the simulation model.

3.3 Solar roof

The roof is modeled by a simple linear model (Innogie 2013) because this work is more focused on the HP/ORC unit. S_{abs} is the total absorber area (150 m²), $\eta_{glazing}$ is the optical efficiency, i.e. the transmissivity, (88%), T_{amb} is the ambient temperature, I is the current solar insolation (in W/m²) and ΔT_{abs} is the difference between the ambient temperature and the average heat transfer fluid temperature in the collector.

$$\dot{Q}_{abs} [W] = S_{abs} (-26.2 - 1.22T_{amb} - 1.7 \Delta T_{abs} + 0.903 I) \quad (1)$$

$$\eta_{abs} [-] = \frac{\dot{Q}_{abs} \cdot \eta_{glazing}}{I \cdot S_{abs}} \quad (2)$$

3.4 Storage

A model of storage including ambient losses (Q_{sto}) is used (Delta calor, 2013). The volume (V_{sto}) and the storage temperature (T_{sto}) are imposed at 1000 litres and 55°C respectively.

$$Q_{sto} \left[\frac{Wh}{day} \right] = 4,2 \cdot V_{sto}^{0,47} \cdot (T_{sto} - T_{amb}) \quad (3)$$

3.5 Pump

Constraints on the flow in ORC mode - relatively high pressure drops (≈ 20 bar) and low flow (≈ 300 g/s) – leads to the use of a volumetric pump. A plunger pump is chosen based on its efficiency, price and tightness. The pump is modeled with a constant isentropic efficiency (ϵ_{is}) of 0.5 (Equation 5). This allows to evaluate the electrical consumption of the pump (\dot{W}_{pp}). \dot{m} is the mass flow, $h_{ex,is}$ is the isentropic enthalpy at the exhaust of the pump and h_{su} is the supply enthalpy of the pump.

$$\epsilon_{is} [-] = \frac{\dot{m} (h_{ex,is} - h_{su})}{\dot{W}_{pp}} \quad (5)$$

4 SIZING

4.1 Definition of the nominal conditions

Since all the components models are detailed, nominal conditions are necessary to size our components. The ORC mode is the one involving the highest heat flow exchanged with the heat source and sink, it is therefore the one selected for the sizing of the system components.

The nominal sizing conditions are defined as follows:

- The evaporating temperature is set to 90°C, which approximately corresponds to the maximum pressure at the inlet of the expander (32 bars) with the selected fluid.
- On the cooling water side, an inlet temperature of 15°C and an outlet temperature of 20°C are assumed.
- The heat source temperature glide, i.e. the difference between the inlet and outlet glycol water temperature on the absorber, is set to 25K in order to conserve a reasonable glycol water flow rate.
- The pinch points are set to 5K for the evaporator and 7.5K for the condenser (Quoilin et al 2011).

- The superheating and sub-cooling of the evaporator and the condenser are set to 10K and 2K respectively.

For the heat pump mode, the following operating conditions are imposed:

- The evaporating temperature (15,7°C) is selected as the equilibrium temperature when the heat pump heating capacity is 8 kWth and when the solar radiation is 90 W/m². This is representative of winter conditions in Denmark.

- The glycol water flow rate (evaporator) is set to the value provided by the ORC mode, depending on the scroll machine power.

- The condensing temperature is fixed to 60°C in order to get a water temperature around 55°C at the inlet of the heat storage (value chosen to be conservative). This temperature is sufficient to cover all the needs of the house.

- For hot water production, a temperature difference of 5K is assumed between the inlet and the outlet of the condenser.

- The superheating and sub-cooling of the evaporator and the condenser are set to 3K and 2K respectively.

The heat exchangers and the pump are sized using the nominal summer conditions. However, the size of the scroll machine (which defines the net power of the system, both in HP and ORC mode) results from a tradeoff between winter and summer performance. This can only be optimized using yearly simulations, as proposed in the section 4.2. The results presented in Table 1 for the nominal conditions have been obtained with the optimal expander size (swept volume = 98.04 cm³) and the optimal fluid (R134a) resulting from yearly simulation optimization (see section 4.2).

Table 1: Nominal conditions

| Mode | Parameter | Value |
|-----------|--------------------------------------|-------|
| Heat pump | Evaporation pressure [bar] | 5 |
| | Condensation pressure [bar] | 17 |
| | Power consumed [W] | 3211 |
| | Mass flow[kg/s] | 0.1 |
| | Compressor isentropic efficiency [%] | 60 |
| | Absorber efficiency [%] | 56 |
| | COP [-] | 4.2 |
| ORC | Evaporation pressure [bar] | 33 |
| | Condensation pressure [bar] | 7 |
| | Power produced [W] | 4733 |
| | Mass flow[kg/s] | 0.3 |
| | Expander isentropic efficiency [%] | 68 |
| | Absorber efficiency [%] | 55 |
| | ORC global efficiency [%] | 7.6 |

4.2 Yearly simulations

In the previous section, the performance of the system has been evaluated on a nominal sizing point, allowing to select and to define the geometry of some components. However when optimizing the design, it is important to account for the performance of the system over a whole year. The system is therefore simulated over a whole year (with one hour time step) by taking into account the average climatic conditions, the average building heat demand for each month of the year and the control strategy. The outside temperature and the solar irradiance are inputs based on Copenhagen since the unit is installed in Denmark. The following control strategy is used: The ORC mode is used as long as the heat storage can

cover the heat demand. If this is not the case, the direct heating mode is activated. Finally, the HP mode is selected for severe climate conditions when the direct heating mode does not allow reaching the required heating temperature.

These simulations allow optimizing discrete variables such as the choice of the working fluid, the use of a recuperator, and the size of the scroll machine (available sizes are taken from the catalog of one manufacturer). The following methodology is applied:

1. For a given configuration (fluid, expander size, recuperator or not), the condenser and of the evaporator are re-sized in term of area and number of plates and the system performance is evaluated over a wide range of evaporation/condensation temperatures, both for the ORC mode and the HP mode. This is done with the nominal condition methodology (see section 4.1).
2. Performance curves are derived from these simulations as a function of the system configuration and of the temperature levels.
3. These curves are implemented in the yearly simulation model, which optimally switches between the three operating modes depending on the weather conditions and on the heat demand.

Point 2 is achieved by running the simulation model for different mean absorber temperatures in order to see the evolution of the electrical power and the heat transfer to the evaporator. In this example, the performance of three compressors (A, B and C) are compared. Technical data is presented in Table 2. This curves are shown for the ORC mode (Figure 3) and for the HP mode (Figure 4).

Table 2: Technical data of the three compressors

| Compressor Parameter | Case A | Case B | Case C |
|------------------------|--------|--------|--------|
| Swept volume [-] | 82.6 | 98.04 | 119.96 |
| Volume ratio [-] | ≈ 3 | ≈ 3 | ≈ 3 |
| Maximum pressure [bar] | 32 | 32 | 32 |

For the ORC mode, the power transferred (\dot{Q}_{ev} continuous line – Figure 3) increases when the mean absorber temperature (\bar{T}) rises and thus net output power (\dot{W}_{net}) increases too. This is due to the fact that the evaporating temperature and pressure increase when the hot source temperature rises, hot source flow rate being constant. However it is important not to exceed the maximum pressure at the expander inlet. This involves a limitation on the power generation. Though, in order to increase the electrical power when the maximum pressure is reached, the pressure is fixed at its maximum value and the super-heating is increased. This explains the discontinuity appearing around 95°C. It can be seen that when the maximum pressure is reached, increasing the superheating involves a decrease in the thermal power transferred (continuous lines) but it allows increasing still a bit more the power produced (dashed lines). From these curves, polynomial laws have been fitted in order to perform the yearly simulation:

$$\dot{Q}_{ev} = C_0 + C_1 \cdot \bar{T} + C_2 \cdot \bar{T}^2 \quad (6)$$

$$\dot{W}_{net} = K_0 + K_1 \cdot \bar{T} + K_2 \cdot \bar{T}^2 \quad (7)$$

For the next step, in the yearly simulation, the mean glycol water temperature will be computed from the weather data (ambient temperature and solar radiation) and from the polynomial expression of the thermal power transferred (Equation 8). This will therefore allow determining the mean absorber temperature corresponding to the weather data and then, the related power generation and the performance of the system in the ORC mode.

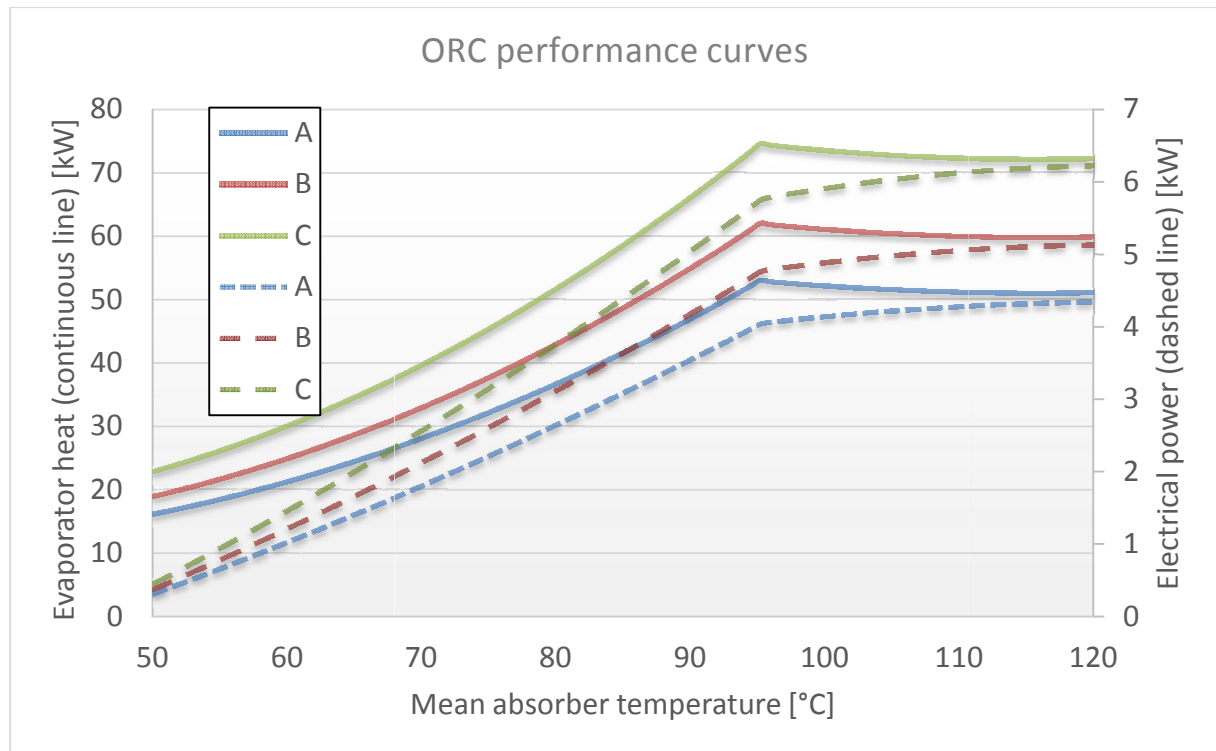


Figure 3: ORC performance curves in function of the mean absorber temperature

In heat pump mode, the sizing of the exchangers is the same as in ORC mode because the thermal power is higher. The simulation model has been run for different mean absorber temperatures in order to see the evolution of the electrical power consumption with the thermal power transferred to the evaporator and operating conditions (Figure 4). The thermal power transferred to the evaporator () and the electrical power consumption () increases when the mean absorber temperature rises. The thermal power recovered at the condenser () increases therefore too because the energy balance on the heat pump gives:

$$(8)$$

Moreover, as the ORC mode, polynomial laws have been derived from these curves for yearly simulations. The weather conditions combined with these polynomial expressions will allow us to determine the mean absorber temperature, the thermal power recovered at the condenser and the performance of the heat pump.

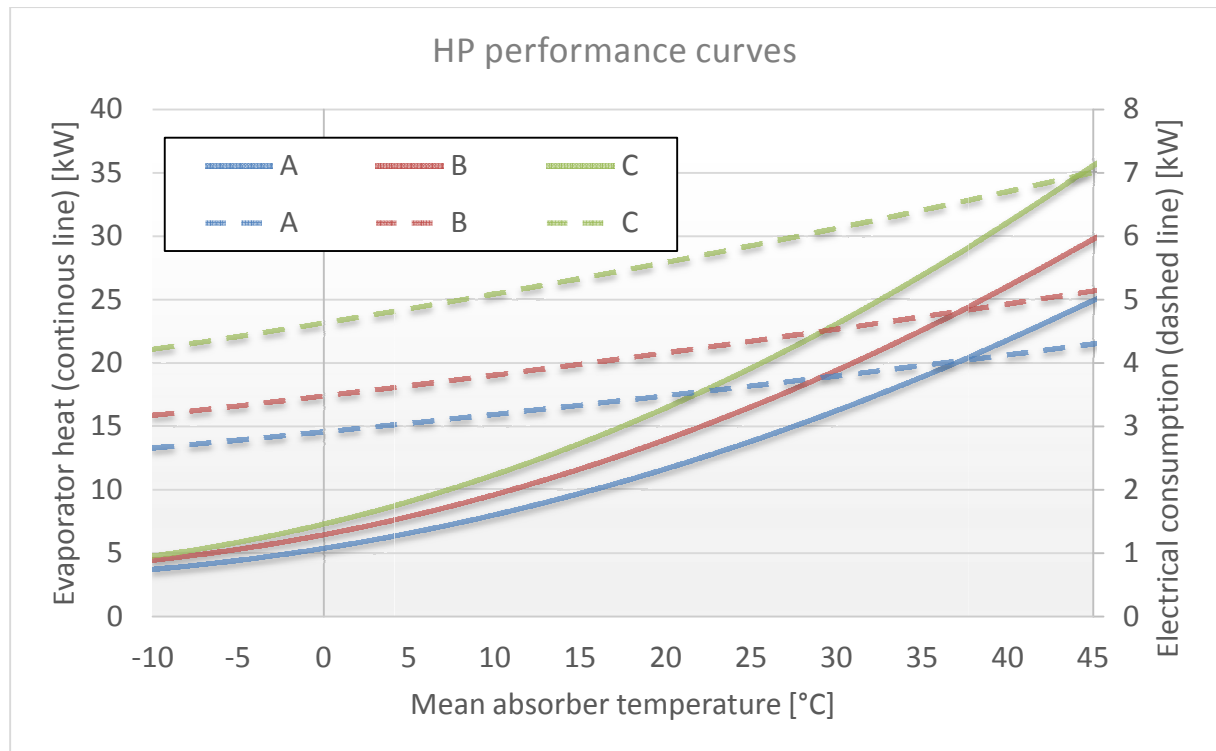


Figure 4: HP performance curves in function of the mean absorber temperature

Finally, the addition of the heat demand of the house and the thermal losses of the heat storage gives the total energy that the unit needs to produce.

Table 3 presents the results in terms of electrical power and running time from these yearly simulation in the case of compressor B and with the optimum fluid (see section 4.3). The heat pump mode is only used during 3 months. The rest of the year, the direct heating is sufficient to provide the heat required by the building and the ORC mode allows producing electricity with the surplus heat.

Table 3: Electrical power and running time for each mode in yearly simulations

| Month | ORC | | HP | | Direct heating |
|-----------|-------------------------|------------------|------------------------------|----------------------|----------------------|
| | Net energy output [kWh] | Running time [h] | Electrical consumption [kWh] | Heating energy [kwh] | Heating energy [kWh] |
| January | - | - | 218.09 | 613.6 (61h) | 515.4 |
| February | 50.8 | 27 | - | - | 1077.6 |
| March | 193.1 | 92 | - | - | 979.2 |
| April | 519.9 | 202 | - | - | 720.5 |
| May | 750.7 | 269 | - | - | 392.3 |
| June | 708.9 | 276 | - | - | 225.3 |
| July | 798.7 | 295 | - | - | 225.3 |
| August | 626.9 | 253 | - | - | 220.2 |
| September | 302.1 | 163 | - | - | 249.5 |
| October | 79.1 | 76 | - | - | 602.4 |
| November | - | - | 3.82 | 12.5 (1h) | 815 |
| December | - | - | 305.4 | 795.6 (89h) | 266.5 |
| Total | 4030.2 | 1653 | 527.3 | 1421.7 | 6289.2 |

4.3 Selection of the fluid

First, R134a has been pre-selected thanks to the Scroll expander operating map (Quoilin 2011). Previous works have examined principal refrigerants appropriate for a low temperature ORC application (Quoilin et al 2011) and suggests those typical fluids: R123, R1234yf, R124, R134a, R152a, R600 and R600a. Each fluid is compared using the yearly simulation and a multi-criteria approach (Quoilin et al 2011). Table 4 shows the annual electrical energy produced and inconvenient for each fluid. Some fluids (R245fa and R123) can be rejected mainly because of the low electrical production. Others presents a significant increase in electrical production (R124, R600, R152a and R600a) but are rejected because of environmental reasons or flammability. The chosen working fluid is thus the R134a although its relatively low performance.

Table 4: Selection of the working fluid

| Fluid | Electrical Production [kWh/year] | GWP [-] | ODP [-] | Inconvenient |
|--------|----------------------------------|---------|---------|-------------------------------------|
| R124 | 5079 | 120 | 0.026 | Environmental reasons |
| R600 | 4239 | 20 | 0 | Flammability |
| R152a | 3969 | 120 | 0 | Flammability |
| R600a | 3814 | 20 | 0 | Flammability |
| R245fa | 3349 | 950 | 0 | Toxicity + low W_{net} |
| R123 | 3105 | 120 | 0.012 | Environment reasons + low W_{net} |
| R134a | 3772 | 1300 | 0 | - |

4.4 Selection of the compressor/expander

The selection of the compressor is done by comparing their electrical production in ORC mode and electrical consumption in HP mode with the refrigerant R134a. Table 5 presents results from yearly simulations with three different compressors with fluid R134a. In ORC mode, compressor B is the best one. This can be explained physically: Too small of a compressor (compressor A for example) leads to a maximum electrical production that limits the performance when large amount of heat are generated in summer. Too large of a compressor leads to low electrical production at part load because it is working mainly at low pressure ratio (zone where the isentropic efficiency is low). In heat pump mode, the same compressor B is the more suited to our application.

Table 5: Selection of the compressor

| Compressor | A | B | C |
|-----------------------------|------|------|------|
| ORC annual production [kWh] | 3834 | 4030 | 3910 |
| HP annual consumption [kWh] | 532 | 527 | 611 |

5 EXPERIMENTATION

5.1 Experimental setup

An experimental study has been carried out on the ORC/HP prototype with refrigerant R134a. Figures 5 presents the detailed scheme of the installation with the refrigerant loop in light blue. The heat source (red) consists of an electrical oil boiler with a maximum output of 150 kW. The condenser is cooled by tap water (light blue).

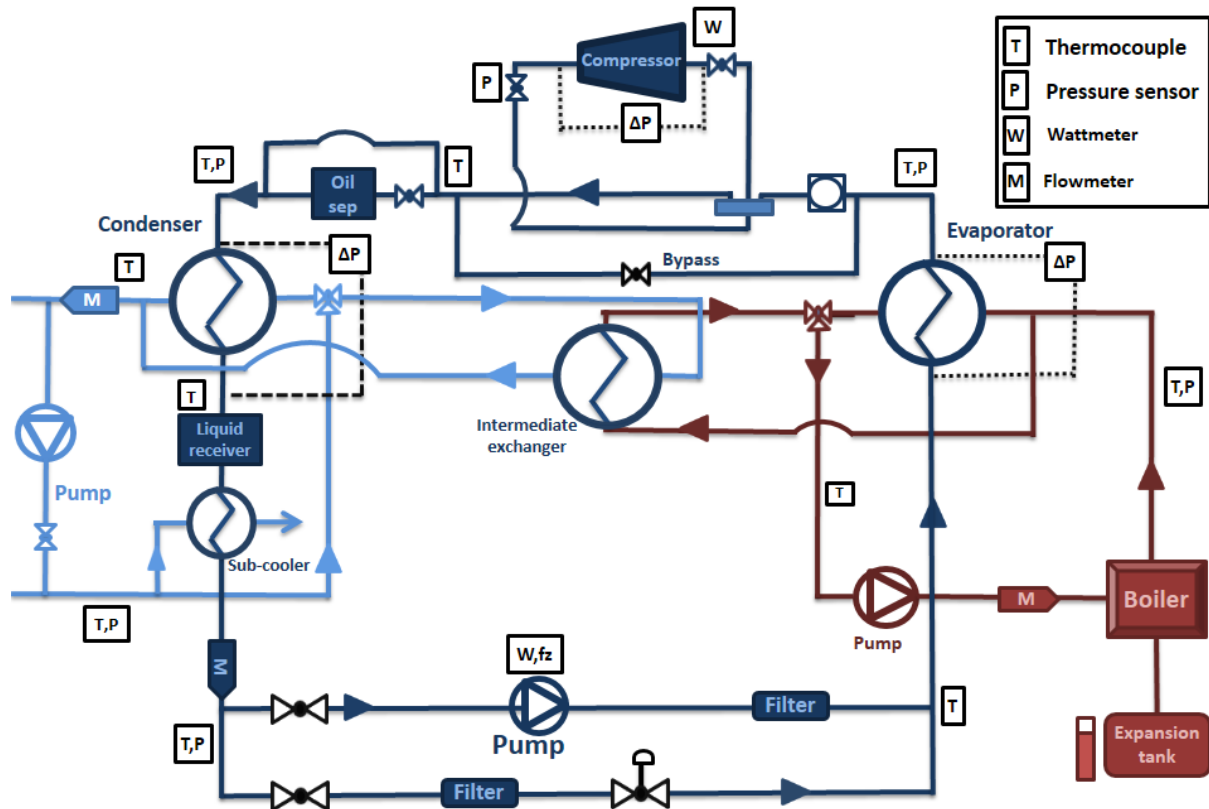


Figure 5: Experimental configuration of the HP/ORC reversible unit

5.2 Experimental results

Experimental results are presented in Table 6. They are compared with theoretical expectations in HP and ORC modes for a similar operating point. First, these results prove the feasibility of such a reversible unit with encouraging performance. However some results are slightly worse than what was expected because of:

- The lower expander isentropic efficiency and high filling factor (i.e. high leakages between high pressure and low pressure).
- The large pressure drop on the four ways valve (up to 4 bars). The four way valve is a component utilized to switch the inlet and outlet of the compressor to commute from one mode to another.
- Necessary sub-cooling to avoid the cavitation of the pump

A higher efficiency of 5.7% is achieved in ORC mode but with lower evaporator power. The efficiency is lower at higher evaporator power because of the high pressure drop on the four ways valve when high flow are needed.

5.3 Improvements

Several improvements are possible:

- Replacing the four ways valve to decrease the pressure drop.
- Controlling the speed of the expander. That will allow to regulate the evaporation temperature and it will therefore allow to optimize the working conditions.
- Developing an expander with an optimized geometry.
- Developing a compressor with a higher maximum admissible pressure (32 bar).
- Using a more efficient pump.

Table 6: Comparison of theoretical and experimental results for two similar operating points (Global efficiency in ORC mode is equal to net electrical production divided by the evaporation heat)

| Mode | Parameter | Nominal theoretical point | Experiment |
|------|-----------------------------|---------------------------|------------|
| ORC | Evaporator power [kW] | 62 | 62 |
| | Evaporation pressure [bar] | 33 | 32 |
| | Condensation pressure [bar] | 7 | 10.3 |
| | Mass flow [g/s] | 300 | 266 |
| | Electrical power [kW] | 4.7 | 3.7 |
| | Global efficiency [%] | 7.5 | 4.2 |
| | Isentropic efficiency [%] | 68 | 58 |
| | Filling factor [-] | 1.019 | 1.12 |
| HP | Condenser power [kW] | 13 | 13.6 |
| | Evaporator pressure [bar] | 5 | 5.7 |
| | Condensation pressure [bar] | 17 | 17.3 |
| | Mass flow [g/s] | 100 | 102 |
| | Electrical power [kW] | 4 | 3.8 |
| | COP [-] | 4.25 | 4.21 |
| | Isentropic efficiency [%] | 60 | 76 |
| | Volumetric efficiency [%] | 91 | 97 |

6 CONCLUSION

This study proposes an innovative reversible domestic HP/ORC system, allowing for both heat and electricity production depending on the weather conditions. A detailed model of the system was built and allowed sizing the components. These simulation also allow us to predict an annual electrical production of 4030 kWh. The electrical consumption in HP mode reach 527.3 kWh over a year. 6289.2 kWh is provided by the direct heating mode. Following that, the technical feasibility of such a reversible unit has been demonstrated. An ORC efficiency of 4.2 is reached and a COP of 4.21 is obtained in conditions comparable to theoretical predictions. Finally, major means to improve the system performance have been pointed out.

After a complete experimental investigation of the unit has been done, the unit is installed and monitored in a house in Herning (Denmark) and some perspectives are listed hereunder:

- Automation of each mode of the unit including control strategies to switch optimally from one mode to another.
- Validation a steady state model of each component and of the global system based on the experimental investigation.
- Evaluation of the performance on yearly simulation based on these experimental validation.
- Creation of a second, more efficient unit.

7 REFERENCES

Delta calor, 2013. "Thermal losses in a storage." http://herve.silve.pagesperso-orange.fr/bilan_th.htm. [accessed January 2014]

European standard European Standards 1999. "Refrigerant compressors - Rating conditions, tolerances and presentation of manufacturer's performance data", DIN EN 12900.

Garcia-Cascales, J.R., Vera-Garcia, F., Corberan-Salvador, J.M., Gonzalez-Macia, J., 2007. "Assessment of boiling and condensation heat transfer correlations in the modelling of plate heat exchangers," *International Journal of Refrigeration*, Vol. 30, pp. 1029-1041.

Hsieh, Y. Y., and Lin, T. F. 2002. "Saturated flow boiling heat transfer and pressure drop of refrigerant R-410A in a vertical plate heat exchanger," *International Journal of Heat and Mass Transfer*, Vol. 45, Part 5, pp. 1033-1044.

Innogie 2013, <http://www.innogie.dk>. [accessed January 2014].

Kuo, W. S., Lie, Y. M., Hsieh, Y. Y., and Lin, T. F. 2005. "Condensation heat transfer and pressure drop of refrigerant R-410A flow in a vertical plate heat exchanger," *International Journal of Heat and Mass Transfer*, Vol. 48, Part 25-26, pp. 5205-5220.

Lemort, V. 2008. "Contribution to the characterization of Scroll machine in compressor and expander modes," PhD. Thesis, University of Liege, Liege.

Lemort, V., Quoilin, S., Cuevas, C., and Lebrun, J. 2009. "Testing and modeling a scroll expander integrated into an Organic Rankine Cycle," *Applied Thermal Engineering*, Vol 29, Part 14–15, pp. 3094-3102.

Lemort, V., Declaye, S., and Quoilin, S., 2011. "Experimental characterization of a hermetic scroll expander for use in a micro-scale Rankine cycle," *Journal of Power and Energy*, Vol. 0, part 0, pp. 1-10.

Pérez-Lombard, L., Ortiz, J., Pout, C. 2008. "A review on buildings energy consumption information," *Energy and building*, Vol. 40, pp. 394-398.

Quoilin, S., 2011. "Sustainable Energy Conversion Through the use of Organic Rankine Cycles for Waste Heat Recovery and Solar Applications," Ph.D. thesis, University of Liege, Liege.

Quoilin, S., Declaye, S., Tchanche, B.F., Lemort, V. 2011. "Thermo-economic optimization of waste heat recovery Organic Rankine Cycles," *Applied Thermal Engineering*, Vol. 31, pp. 2885-2893.

Schimpf, S., Span, R. (2013) "Combining a thermally supported ground source heat pump with an ORC process." Draft for an oral session at the 2nd ORC conference 2013.

Thonon B., 1995. "Recent research and developments in plate heat exchangers," *Fuel and Energy Abstracts*, Vol. 36, Part 5, pp. 361.